



University
of Ferrara



FTE@LHC & NLOAccess STRONG 2020 joint kick-off meeting
CERN – November 7-8 2019

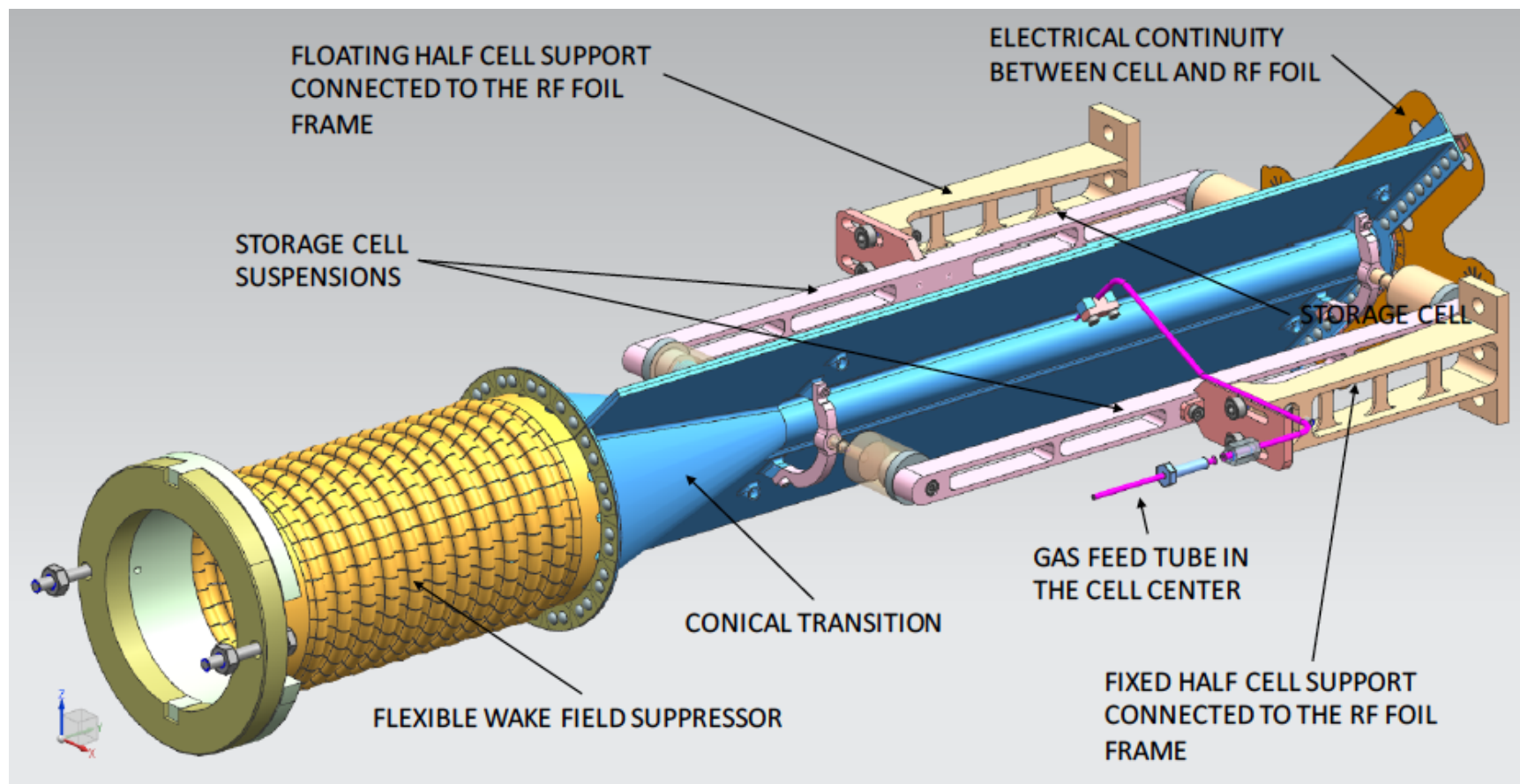
Status and prospects with the unpolarised (SMOG2) and polarized (LHCSpin) targets

Luciano L. Pappalardo (for the proponents)
pappalardo@fe.infn.it

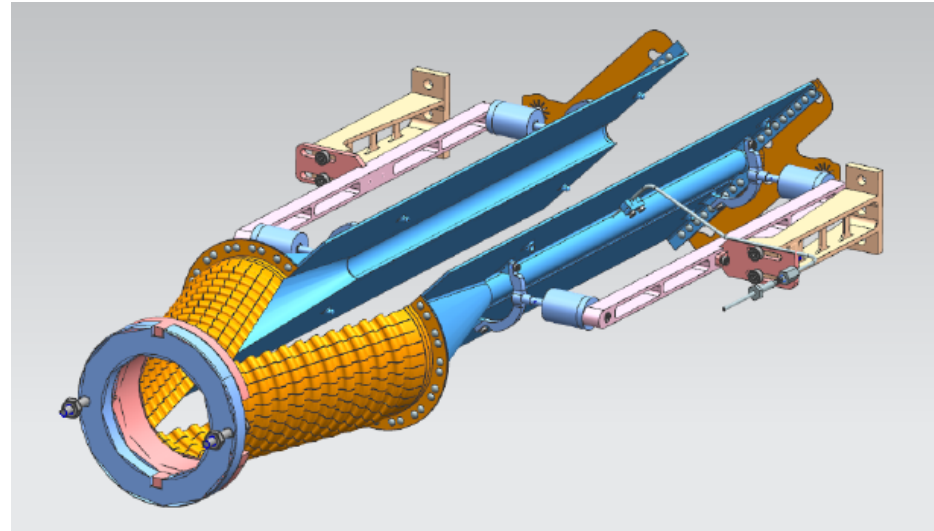
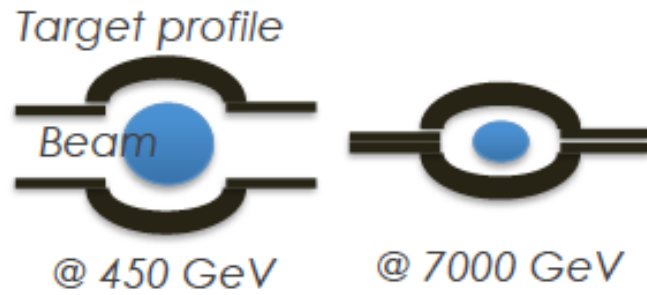
The SMOG upgrade (SMOG2)

The SMOG2 setup

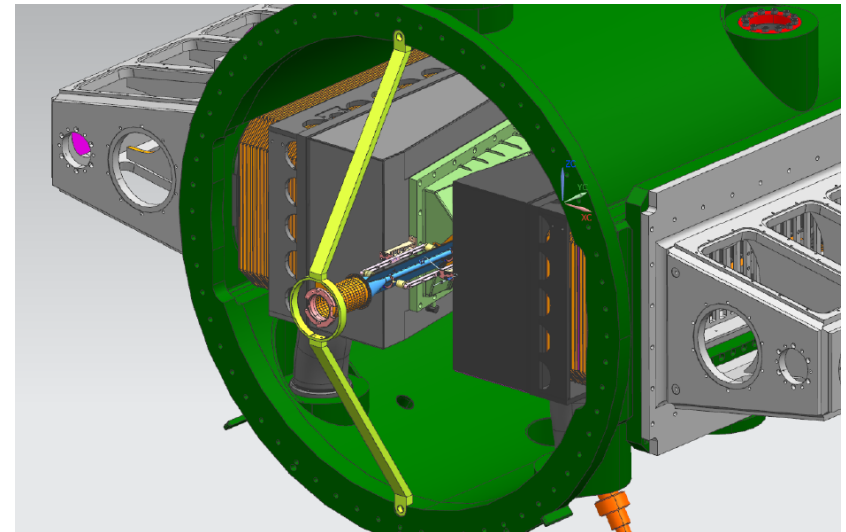
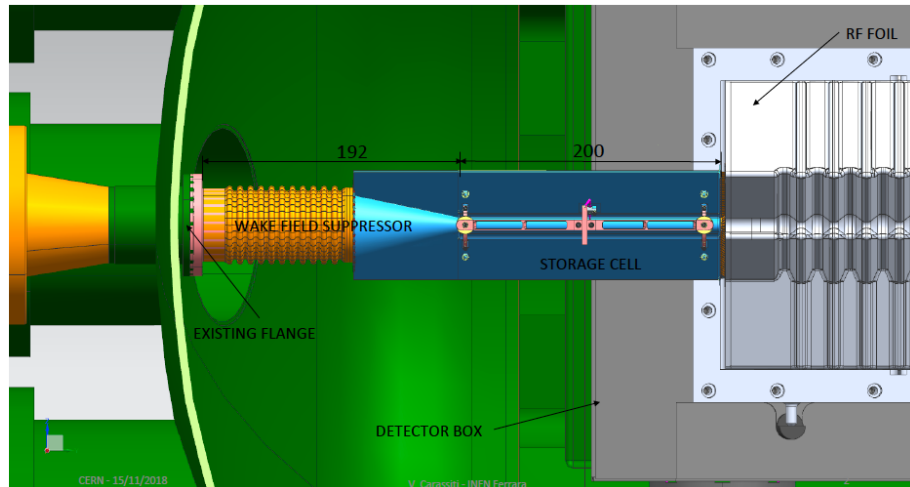
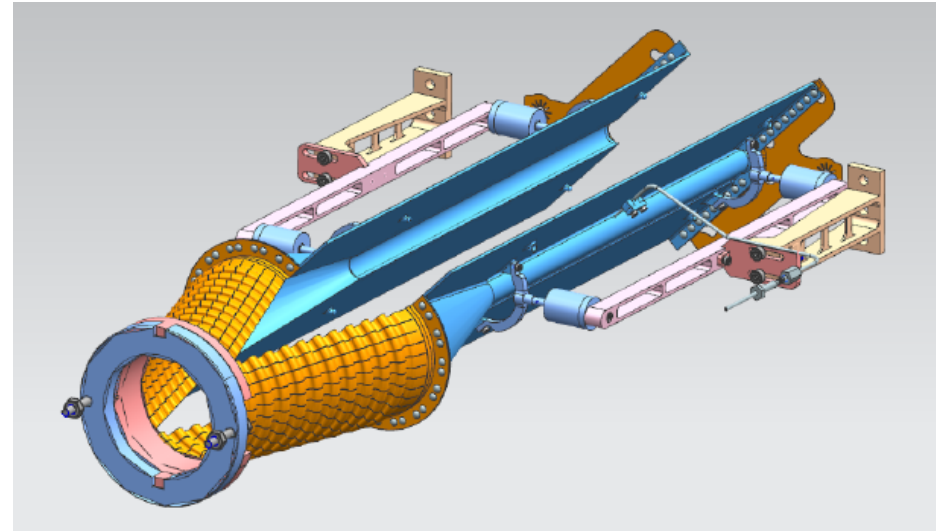
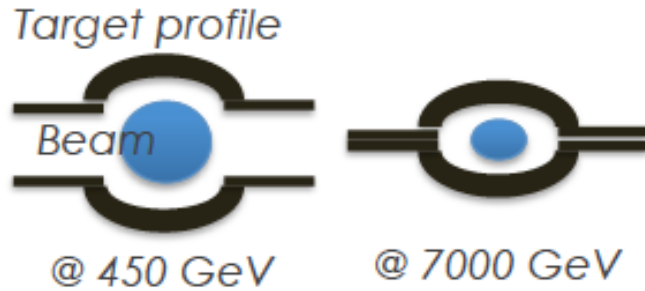
The core of the SMOG2 upgrade is the use of a 20cm long **storage cell** for the target gas to be installed in front of the VELO



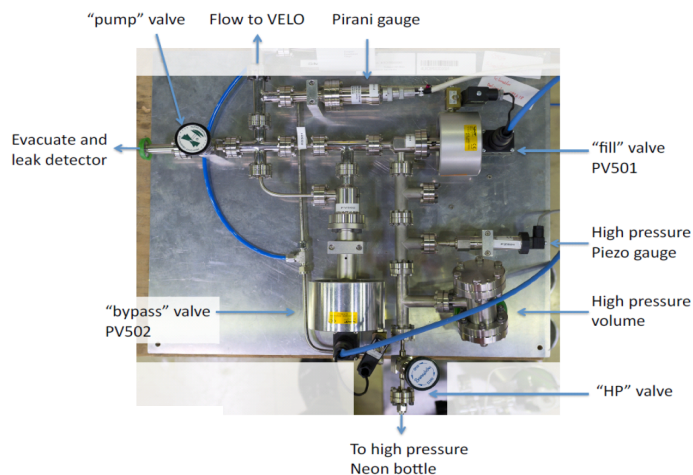
The SMOG2 setup



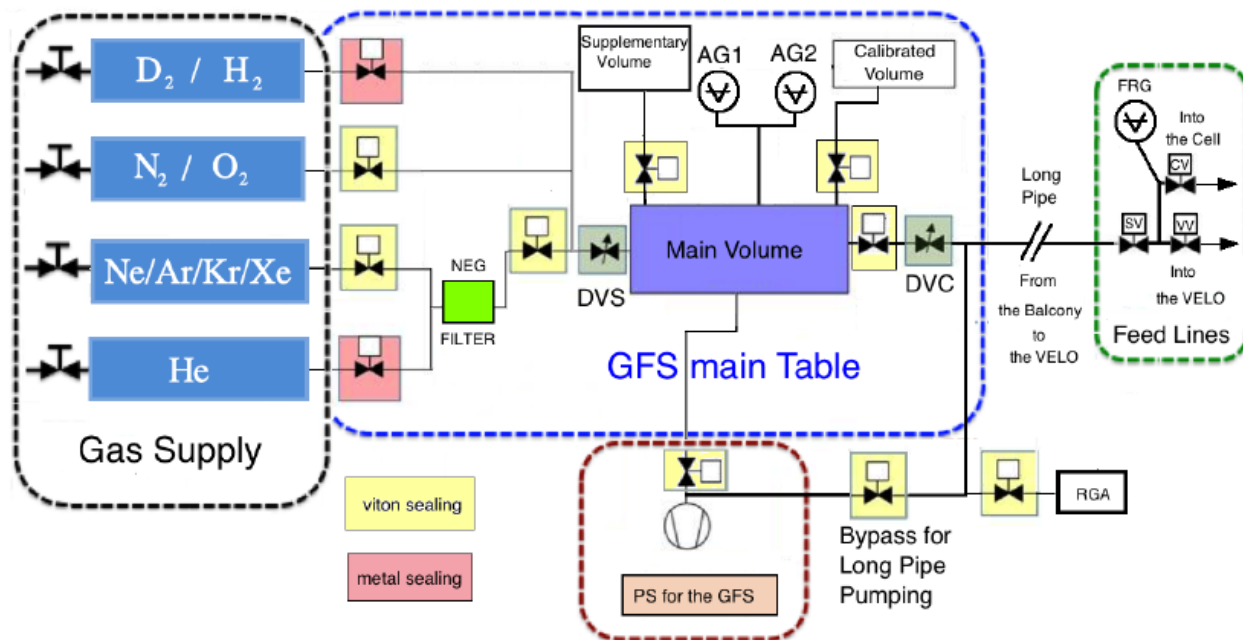
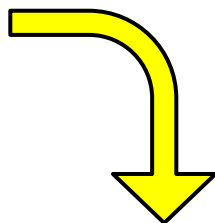
The SMOG2 setup



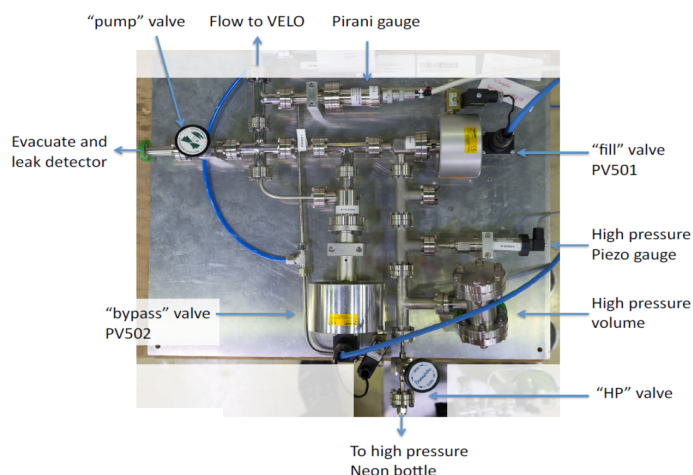
The SMOG2 setup



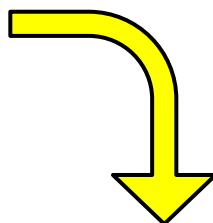
SMOG Gas Feed System



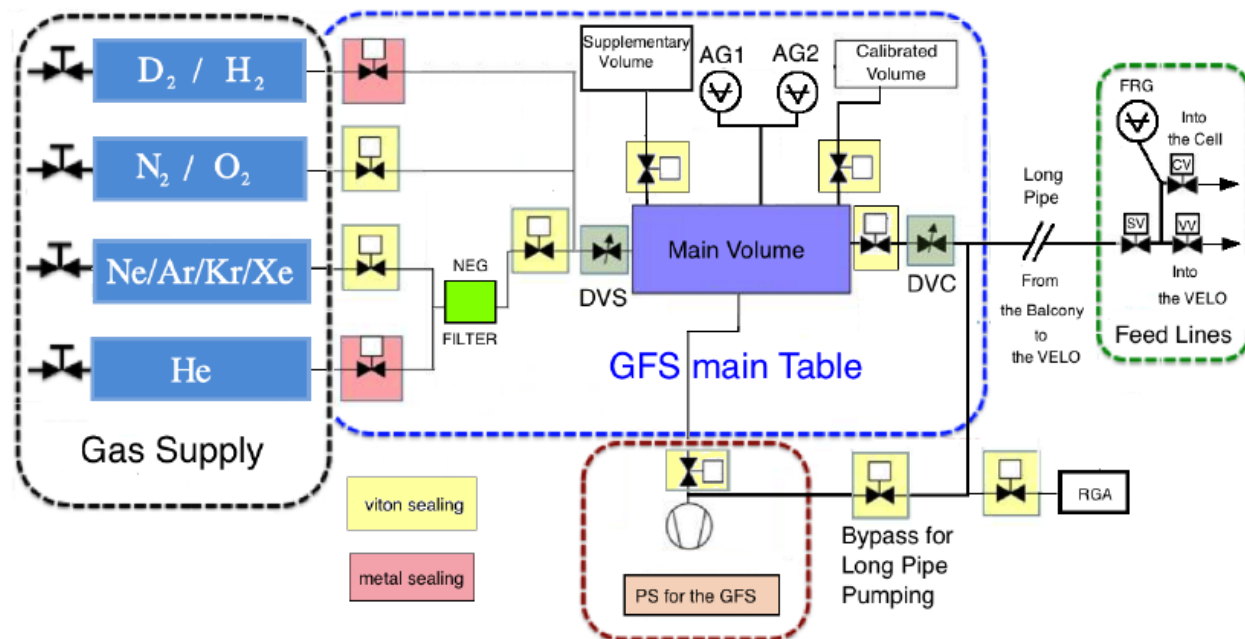
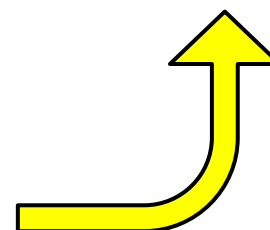
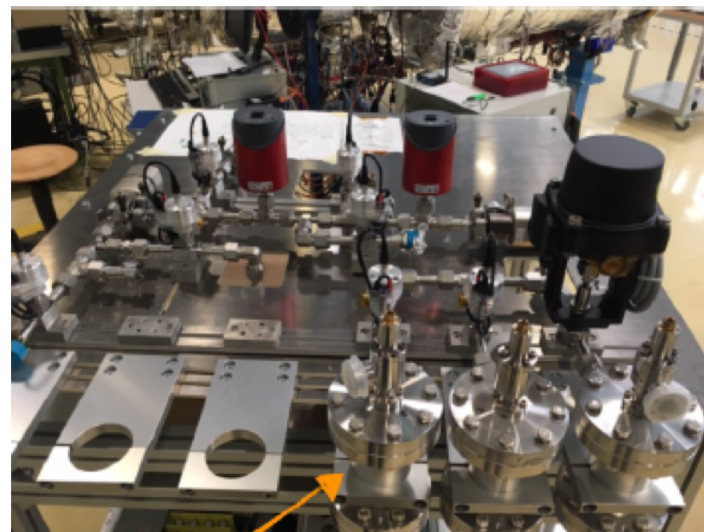
The SMOG2 setup



SMOG Gas Feed System



SMOG2 Gas Feed System
(under construction)



SMOG2 vs. SMOG

- ✓ **Increase of target density (luminosity)**
by a factor 10-35 (depending on the gas type) using the same gas load of SMOG

Gas	Increase in luminosity SMOG2/SMOG
He	10.9
Ne	24.4
Ar	34.5

SMOG2 vs. SMOG

- ✓ **Increase of target density (luminosity)**
by a factor 10-35 (depending on the gas type) using the same gas load of SMOG

Gas	Increase in luminosity SMOG2/SMOG
He	10.9
Ne	24.4
Ar	34.5

- ✓ Possibility to inject **more gas species**: H, D, He, N, O, Ne, Ar, Kr, Xe (SMOG: He, Ne, Ar)
 - H, D \Rightarrow study of TMDs/GPDs through unpolarized observables
 - N, O \Rightarrow relevant for atmospheric CR

SMOG2 vs. SMOG

- ✓ **Increase of target density (luminosity)**
by a factor 10-35 (depending on the gas type) using the same gas load of SMOG

Gas	Increase in luminosity SMOG2/SMOG
He	10.9
Ne	24.4
Ar	34.5

- ✓ Possibility to inject **more gas species**: H, D, He, N, O, Ne, Ar, Kr, Xe (SMOG: He, Ne, Ar)
 - H, D \Rightarrow study of TMDs/GPDs through unpolarized observables
 - N, O \Rightarrow relevant for atmospheric CR
- ✓ **More sophisticated Gas Feed System**: will allow to measure the target density (and luminosity) with much higher precision (few percent level) \Rightarrow **better accuracy on absolute cross sections**
- ✓ Well **defined interaction region** upstream of the collider IP (limited to cell length: 20 cm)

SMOG2 vs. SMOG

- ✓ **Increase of target density (luminosity)**
by a factor 10-35 (depending on the gas type) using the same gas load of SMOG

Gas	Increase in luminosity SMOG2/SMOG
He	10.9
Ne	24.4
Ar	34.5

- ✓ Possibility to inject **more gas species**: H, D, He, N, O, Ne, Ar, Kr, Xe (SMOG: He, Ne, Ar)
 - H, D \Rightarrow study of TMDs/GPDs through unpolarized observables
 - N, O \Rightarrow relevant for atmospheric CR
- ✓ **More sophisticated Gas Feed System**: will allow to measure the target density (and luminosity) with much higher precision (few percent level) \Rightarrow **better accuracy on absolute cross sections**
- ✓ Well **defined interaction region** upstream of the collider IP (limited to cell length: 20 cm)
- ✓ **Installation in the next months**
 - Nov 2019 Coating
 - Dec 2019 Pre-installation (surface lab) and alignment
 - Jan 2020 Installation in the pit
- ✓ Data-taking starts in 2021 (Run 3)

Data-taking scenarios

- Fixed-target data-taking must not affect the core LHCb pp program
- In Run 3 a **new (very challenging) online reconstruction strategy** will be adopted:
 - full detector readout at 40 MHz
 - real time reconstruction and selection at 30 MHz (with average 5 pp collisions per bunch-crossing)

Data-taking scenarios

- Fixed-target data-taking must not affect the core LHCb pp program
- In Run 3 a **new (very challenging) online reconstruction strategy** will be adopted:
 - full detector readout at 40 MHz
 - real time reconstruction and selection at 30 MHz (with average 5 pp collisions per bunch-crossing)
- **Three possible strategies:**
 1. **Dedicated runs** (à-la SMOG)
 - simpler trigger implementation (decouple pp and FT physics)
 - but very limited running time (low statistics)

Data-taking scenarios

- Fixed-target data-taking must not affect the core LHCb pp program
- In Run 3 a **new (very challenging) online reconstruction strategy** will be adopted:
 - full detector readout at 40 MHz
 - real time reconstruction and selection at 30 MHz (with average 5 pp collisions per bunch-crossing)
- **Three possible strategies:**
 1. **Dedicated runs** (à-la SMOG)
 - simpler trigger implementation (decouple pp and FT physics)
 - but very limited running time (low statistics)
 2. **Simultaneous run, FT physics only with beam1 non-colliding bunches**
 - simpler trigger implementation (decouple pp and FT physics)
 - but exploit only 10-20% of bunches
 - but can produce some background to pp physics

Data-taking scenarios

- Fixed-target data-taking must not affect the core LHCb pp program
- In Run 3 a **new (very challenging) online reconstruction strategy** will be adopted:
 - full detector readout at 40 MHz
 - real time reconstruction and selection at 30 MHz (with average 5 pp collisions per bunch-crossing)
- **Three possible strategies:**
 1. **Dedicated runs** (à-la SMOG)
 - simpler trigger implementation (decouple pp and FT physics)
 - but very limited running time (low statistics)
 2. **Simultaneous run, FT physics only with beam1 non-colliding bunches**
 - simpler trigger implementation (decouple pp and FT physics)
 - but exploit only 10-20% of bunches
 - but can produce some background to pp physics
 3. **Simultaneous run, FT physics only with all bunches**
 - maximize FT physics output for a given gas flow
 - but requires merging FT and pp physics requirements for online reco and trigger
 - but can produce some background to pp physics (and vice-versa)

Real-time reconstruction of FT events

Work in progress to realize the third scenario

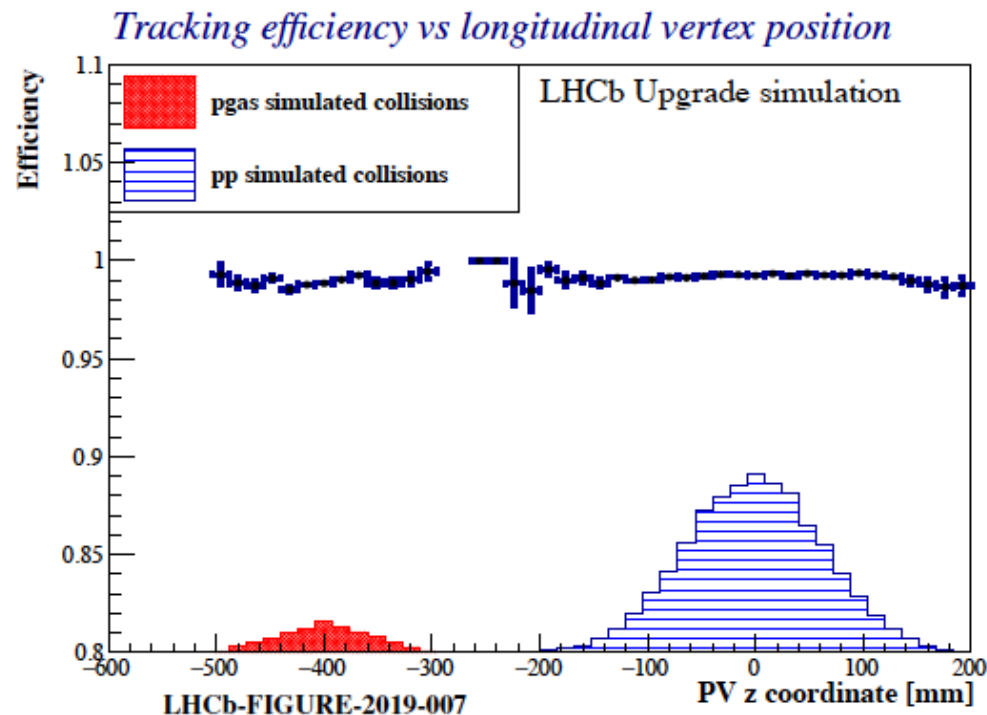
- Fit FT physics in the trigger data bandwidth
- Study additional backgrounds from FT events on pp physics and vice-versa

Real-time reconstruction of FT events

Work in progress to realize the third scenario

- Fit FT physics in the trigger data bandwidth
- Study additional backgrounds from FT events on pp physics and vice-versa

Some promising results have already been achieved



SMOG2 projected performances for LHC Run3

LHCb-PUB-2018-015

System	$\sqrt{s_{NN}}$ (GeV)	$\langle \text{pressure} \rangle$ (10^{-5} mbar)	ρ_S (cm^{-2})	\mathcal{L} ($\text{cm}^{-2}\text{s}^{-1}$)	Rate (MHz)	Time (s)	$\int \mathcal{L}$ (pb^{-1})
$p\text{H}_2$	115	4.0	2.0×10^{13}	6×10^{31}	4.6	2.5×10^6	150
$p\text{D}_2$	115	2.0	1.0×10^{13}	3×10^{31}	4.3	0.3×10^6	9
$p\text{Ar}$	115	1.2	0.6×10^{13}	1.8×10^{31}	11	2.5×10^6	45
$p\text{Kr}$	115	0.8	0.4×10^{13}	1.2×10^{31}	12	2.5×10^6	30
$p\text{Xe}$	115	0.6	0.3×10^{13}	0.9×10^{31}	12	2.5×10^6	22
$p\text{He}$	115	2.0	1.0×10^{13}	3×10^{31}	3.5	3.3×10^3	0.1
$p\text{Ne}$	115	2.0	1.0×10^{13}	3×10^{31}	12	3.3×10^3	0.1
$p\text{N}_2$	115	1.0	0.5×10^{13}	1.5×10^{31}	9.0	3.3×10^3	0.1
$p\text{O}_2$	115	1.0	0.5×10^{13}	1.5×10^{31}	10	3.3×10^3	0.1
PbAr	72	8.0	4.0×10^{13}	1×10^{29}	0.3	6×10^5	0.060
PbH_2	72	8.0	4.0×10^{13}	1×10^{29}	0.2	1×10^5	0.010

Assumptions:

- Parallel beam-gas and beam-beam data taking for 1/3 of total beam time
- Use of all beam bunches for fixed-target physics
- Beam intensity of 2.6×10^{14} protons (2.2×10^{11} Pb ions)
- Average pressure assuming $< 5\%$ of expected rate of pp collisions per bunch crossing

SMOG2 projected performances for LHC Run3

LHCb-PUB-2018-015

System	$\sqrt{s_{NN}}$ (GeV)	< pressure> (10^{-5} mbar)	ρ_S (cm^{-2})	\mathcal{L} ($\text{cm}^{-2}\text{s}^{-1}$)	Rate (MHz)	Time (s)	$\int \mathcal{L}$ (pb^{-1})
$p\text{H}_2$	115	4.0	2.0×10^{13}	6×10^{31}	4.6	2.5×10^6	150
$p\text{D}_2$	115	2.0	1.0×10^{13}	3×10^{31}	4.3	0.3×10^6	9
$p\text{Ar}$	115	1.2	0.6×10^{13}	1.8×10^{31}	11	2.5×10^6	45
$p\text{Kr}$	115	0.8	0.4×10^{13}	1.2×10^{31}	12	2.5×10^6	30
$p\text{Xe}$	115	0.6	0.3×10^{13}	0.9×10^{31}	12	2.5×10^6	22

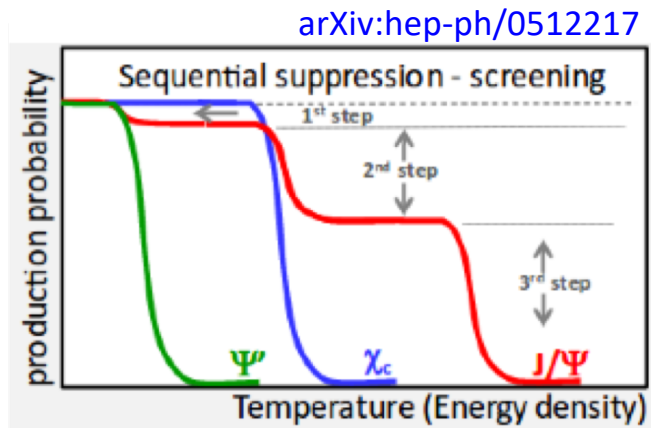
	SMOG published result $p\text{He}@87$ GeV	SMOG largest sample $p\text{Ne}@69$ GeV	SMOG2 example $p\text{Ar}@115$ GeV
Integrated luminosity	7.6 nb^{-1}	$\sim 100 \text{ nb}^{-1}$	$\sim 45 \text{ pb}^{-1}$
syst. error on J/ψ x-sec.	7%	6 - 7%	2 - 3 %
J/ψ yield	400	15k	15M
D^0 yield	2000	100k	150M
Λ_c^+ yield	20	1k	1.5M
$\psi(2S)$ yield	negl.	150	150k
$\Upsilon(1S)$ yield	negl.	4	7k
Low-mass Drell-Yan yield	negl.	5	9k

Opportunities with SMOG2: heavy-ion physics

- New measurements of prompt charm production with a significantly increased statistical power. New measurements can include also **charmed baryons** (e.g. Λ_c^+ , Σ_c^+).

Opportunities with SMOG2: heavy-ion physics

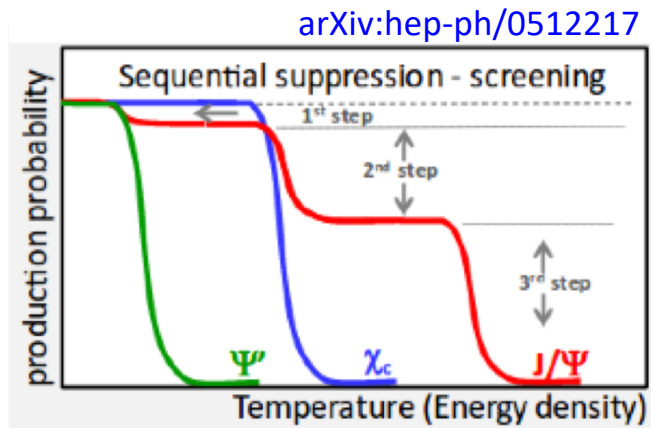
- New measurements of prompt charm production with a significantly increased statistical power. New measurements can include also **charmed baryons** (e.g. Λ_c^+ , Σ_c^+).
- Measurements can be extended to charmonium excited states. Relevant for studying the **sequential charmonia suppression** in Pb-A collisions



(different binding energies lead to different dissociation temperatures)

Opportunities with SMOG2: heavy-ion physics

- New measurements of prompt charm production with a significantly increased statistical power. New measurements can include also **charmed baryons** (e.g. Λ_c^+ , Σ_c^+).
- Measurements can be extended to charmonium excited states. Relevant for studying the **sequential charmonia suppression** in Pb-A collisions

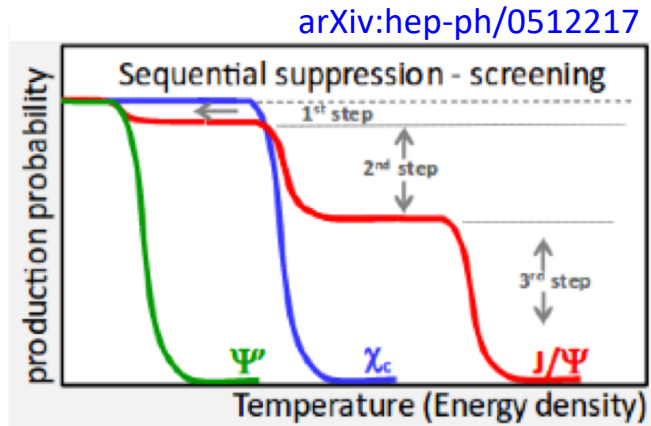


(different binding energies lead to different dissociation temperatures)

- Possibility to measure **prompt beauty production** (7k reconstructed $\Upsilon(1S) \rightarrow \mu^+ \mu^-$ events are foreseen with $\mathcal{L} \sim 45 \text{ pb}^{-1}$ in pAr collisions)

Opportunities with SMOG2: heavy-ion physics

- New measurements of prompt charm production with a significantly increased statistical power. New measurements can include also **charmed baryons** (e.g. Λ_c^+ , Σ_c^+).
- Measurements can be extended to charmonium excited states. Relevant for studying the **sequential charmonia suppression** in Pb-A collisions



(different binding energies lead to different dissociation temperatures)

- Possibility to measure **prompt beauty production** (7k reconstructed $\Upsilon(1S) \rightarrow \mu^+ \mu^-$ events are foreseen with $\mathcal{L} \sim 45 \text{ pb}^{-1}$ in pAr collisions)
- Measurement of QGP-related flow observables and correlations in Pb-A collisions at $\sqrt{s_{NN}} \sim 70 \text{ GeV}$

Opportunities with SMOG2: cosmic rays and DM

- Extend the present antiproton production measurement to include **production of antiprotons from anti-hyperon decays (e.g., $\bar{\Lambda}$, $\bar{\Sigma}$)**

Opportunities with SMOG2: cosmic rays and DM

- Extend the present antiproton production measurement to include **production of antiprotons from anti-hyperon decays (e.g., $\bar{\Lambda}$, $\bar{\Sigma}$)**
- Thanks to the possibility to use also a H_2 (and D_2) target, it will be possible to precisely measure the ratio:

$$\frac{\sigma(pHe \rightarrow \bar{p}X)}{\sigma(pp \rightarrow \bar{p}X)}$$

where many systematic uncertainties cancel

Opportunities with SMOG2: cosmic rays and DM

- Extend the present antiproton production measurement to include **production of antiprotons from anti-hyperon decays (e.g., $\bar{\Lambda}$, $\bar{\Sigma}$)**
- Thanks to the possibility to use also a H_2 (and D_2) target, it will be possible to precisely measure the ratio:

$$\frac{\sigma(pHe \rightarrow \bar{p}X)}{\sigma(pp \rightarrow \bar{p}X)}$$

where many systematic uncertainties cancel

- ...and also:

$$\frac{\sigma(pd \rightarrow \bar{p}X)}{\sigma(pp \rightarrow \bar{p}X)}$$

which can provide constraints on

$$\frac{\sigma(pp \rightarrow \bar{n}X)}{\sigma(pp \rightarrow \bar{p}X)}$$

Opportunities with SMOG2: cosmic rays and DM

- Extend the present antiproton production measurement to include **production of antiprotons from anti-hyperon decays (e.g., $\bar{\Lambda}$, $\bar{\Sigma}$)**
- Thanks to the possibility to use also a H_2 (and D_2) target, it will be possible to precisely measure the ratio:

$$\frac{\sigma(pHe \rightarrow \bar{p}X)}{\sigma(pp \rightarrow \bar{p}X)}$$

where many systematic uncertainties cancel

- ...and also:

$$\frac{\sigma(pd \rightarrow \bar{p}X)}{\sigma(pp \rightarrow \bar{p}X)}$$

which can provide constraints on

$$\frac{\sigma(pp \rightarrow \bar{n}X)}{\sigma(pp \rightarrow \bar{p}X)}$$

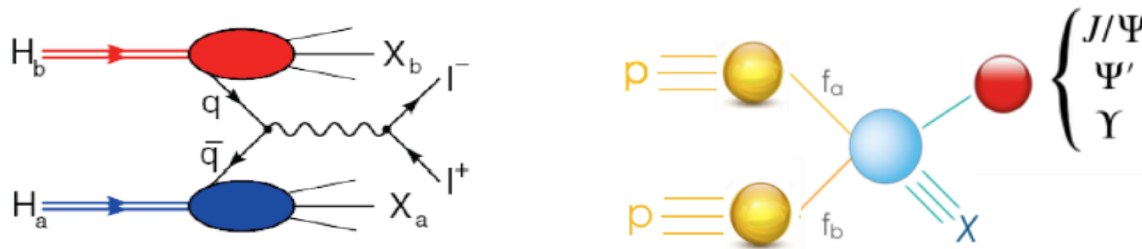
- Explore the possibility to measure **production of light anti-nuclei (\bar{d} , $\overline{{}^3\text{He}}$, $\overline{{}^4\text{He}}$)**

Opportunities with SMOG2: nucleon structure

- SMOG2 operated with H_2 and D_2 targets offers unique conditions to probe quark and gluon PDFs in nucleons and nuclei, especially at high- x and moderately-high Q^2 , where present experimental data are largely insufficient to constraint the theoretical distributions.

Opportunities with SMOG2: nucleon structure

- SMOG2 operated with H_2 and D_2 targets offers unique conditions to probe quark and gluon PDFs in nucleons and nuclei, especially at high- x and moderately-high Q^2 , where present experimental data are largely insufficient to constraint the theoretical distributions.
- Measurements of **quark and gluon transverse-momentum-dependent (TMD) PDFs**, respectively in Drell-Yan and inclusive production of quarkonia (J/ψ , ψ' , Υ , etc.), will significantly improve our understanding of the 3D structure of the nucleon in the non-perturbative regime of QCD.



...find a lot more in back-up slides

From SMOG2 to the polarized target



LHC

EDMS NO. 2085258	REV. 0.2	VALIDITY DRAFT
REFERENCE LHC-X8FTS-EC-0001		

Date: 2019-07-19

ENGINEERING CHANGE REQUEST

SMOG2

BRIEF DESCRIPTION OF THE PROPOSED CHANGE(S):

LHCb proposes an upgraded version of the existing gas injection system SMOG. The core idea of the project, called SMOG2, is the use of a storage cell for the injected gas to be installed upstream of the VELO detector. The main advantage of the proposed system is to increase by up to two orders of magnitude the effective target areal density, thus resulting in a significant increase of the luminosity for fixed-target collisions, keeping the same gas flow rate used up to now with SMOG.

DOCUMENT PREPARED BY:

Pasquale Di Nezza EP-ULB
Vittore Carassiti EP-ULB
Giuseppe Ciullo EP-ULB
Luciano Pappalardo EP-ULB
Paolo Lenisa (Univ. Ferrara and
INFN)
Erhard Steffens (Univ. Erlangen)

DOCUMENT TO BE CHECKED BY:

C. Adorisio, G. Arduini, M. Barberan,
M. Bernardini, G. Bregliozzi,
R. Bruce, R. de Maria,
M. Ferro-Luzzi, R. Folini,
C. Gaignant, J.-C. Gaye,
M. Giordano,
G. Iadecola, J. Jansant,
A. Marz, P. Muto, M. Pozzi,
B. Salvani, J. Sestak,
J. Volpert, J. Wenginger,
J. Wollmann

MENT TO BE APPROVED BY:

P. Collier
(on behalf of LMC)

Rolf Lindner
(LHCb Technical Coordinator)

DOCUMENT SENT FOR INFORMATION TO:

Giovanni Passalev

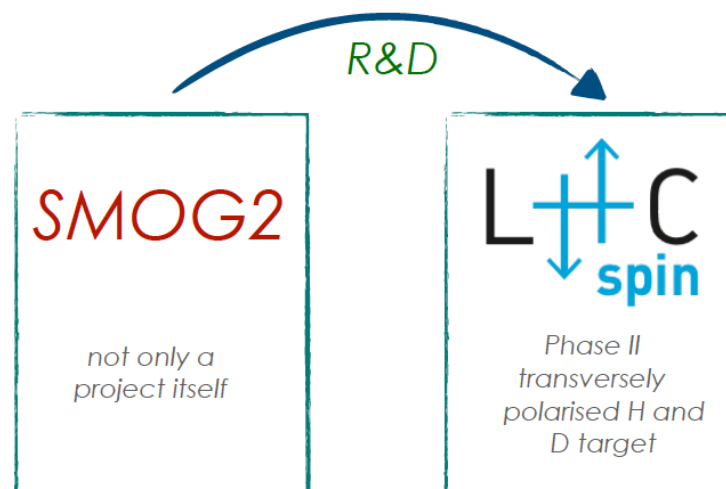
SUMMARY OF THE ACTIONS TO BE UNDERTAKEN:

- Installation of an openable storage cell, fixed to the VELO rf-box frame
- Installation of a 4" gas pipe line into the P8 cavern
- Replacement of the SMOG Gas Feed System located into the P8 cavern

Note: When approved, an Engineering Change Request becomes an Engineering Change Order.

This document is uncontrolled when printed. Check the EPMS to verify that this is the correct version before use.

- The approval of SMOG2, opens the way for a **future HERMES-like polarized gas target at LHCb (LHCspin project)**



- Several SMOG2 approved solutions are common to the polarized target case
- R&D for the polarized target has started
- Proposed installation during LS3

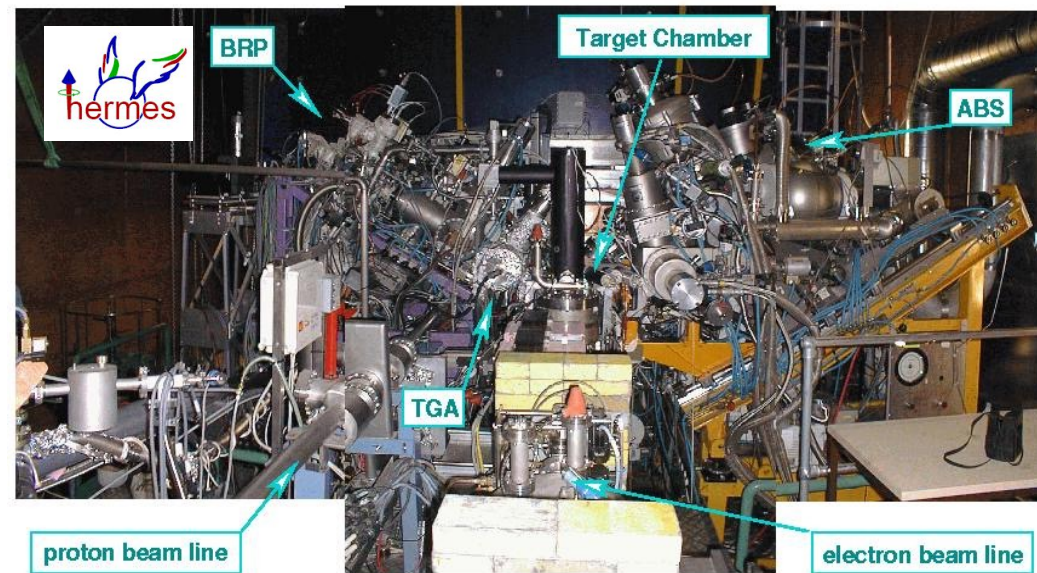
The LHCspin project

- ✓ **Broad variety of possible reactions:**
 - polarized: pp^\uparrow , pd^\uparrow
 - unpolarized: pA , PbA ($A=H, D, He, O, Ne, Ar, Kr, Xe$)
- ✓ **Polarized gas target technology well established (10 years @ HERMES)**
Very high performances ($P \sim 80\%$)
- ✓ **Marginal impact on LHC beam and mainstream physics at current experiments**
- ✓ **Broad physics program (details in backup slides)**

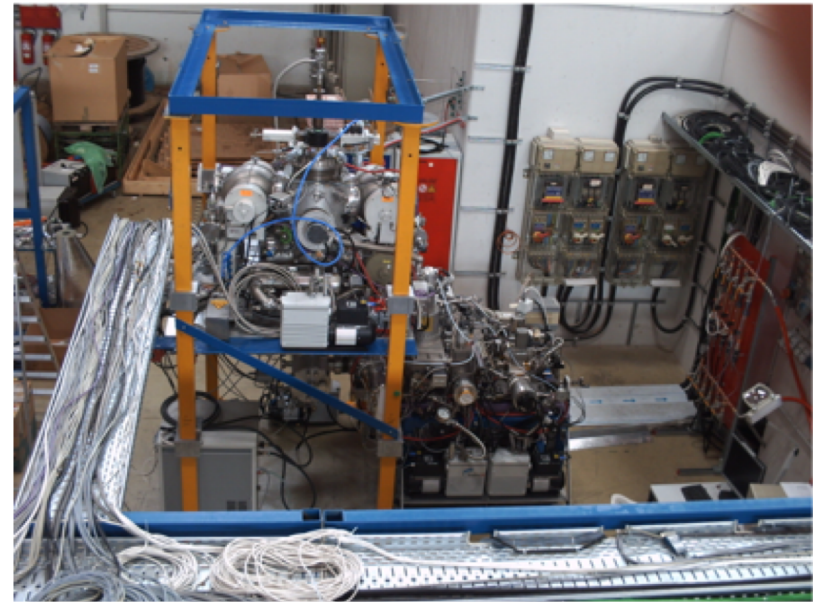
The HERMES-like polarized target concept

The technique proposed is well consolidated

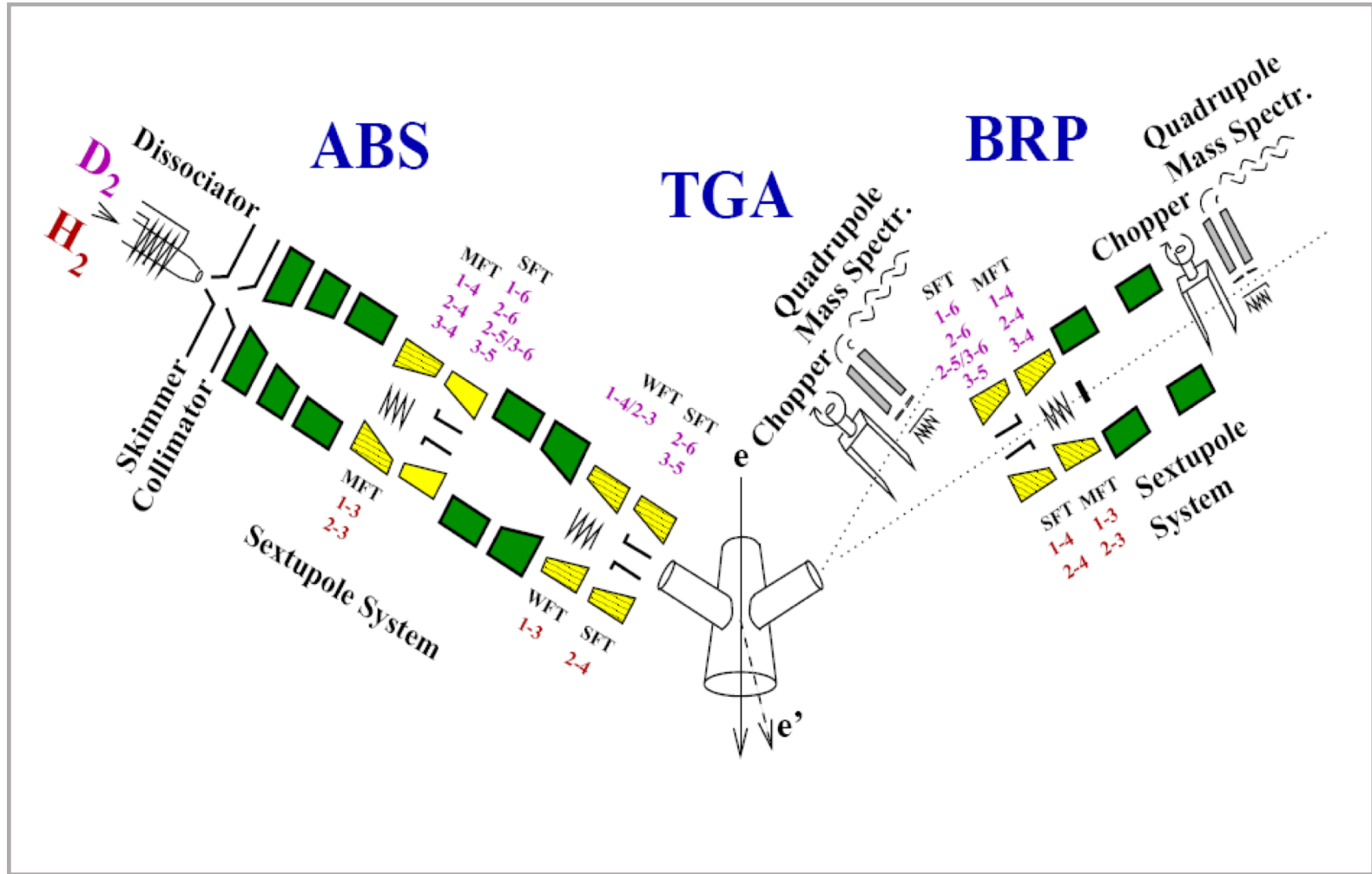
HERMES setup



Jülich setup (II generation)



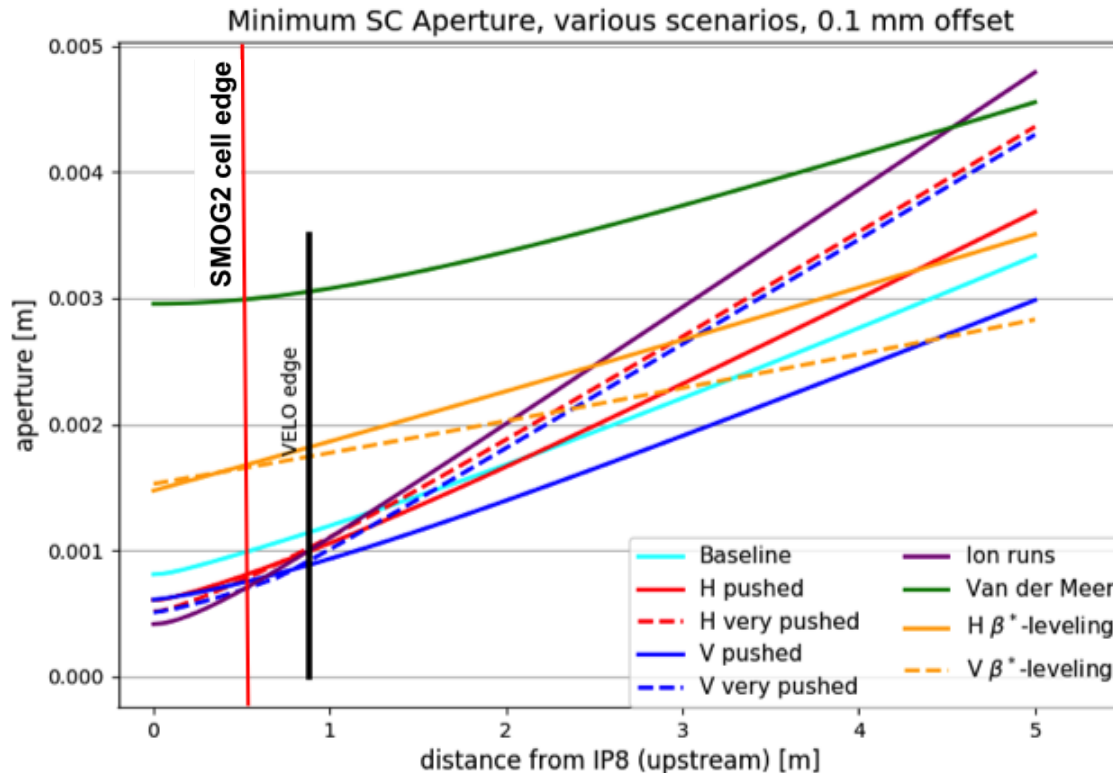
The HERMES-like polarized target concept



Minimal requirements for a PGT at LHC

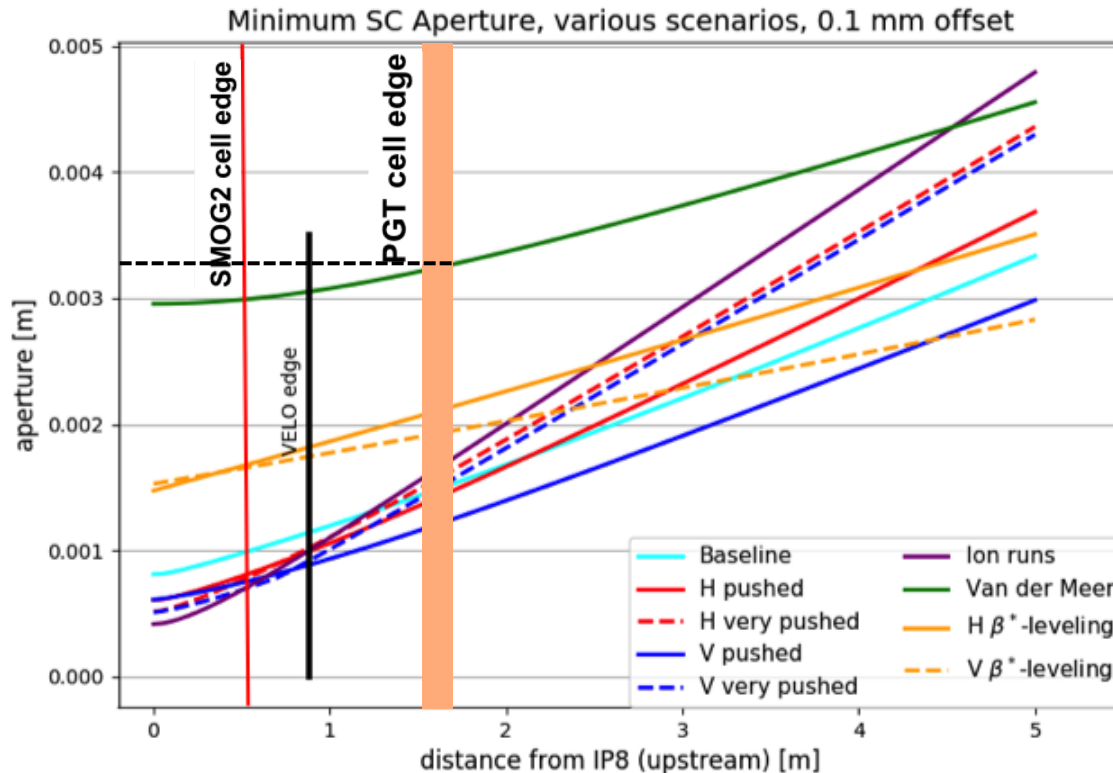
1. Beam size and cell opening

- The achievable luminosity critically depends on the geometry of the storage cell:
 $L \propto D^{-3} \Rightarrow$ **smaller diameter** \Leftrightarrow **higher luminosity**
- The cell aperture (diameter) must comply with the beam size in the stability region (dynamic aperture)



1. Beam size and cell opening

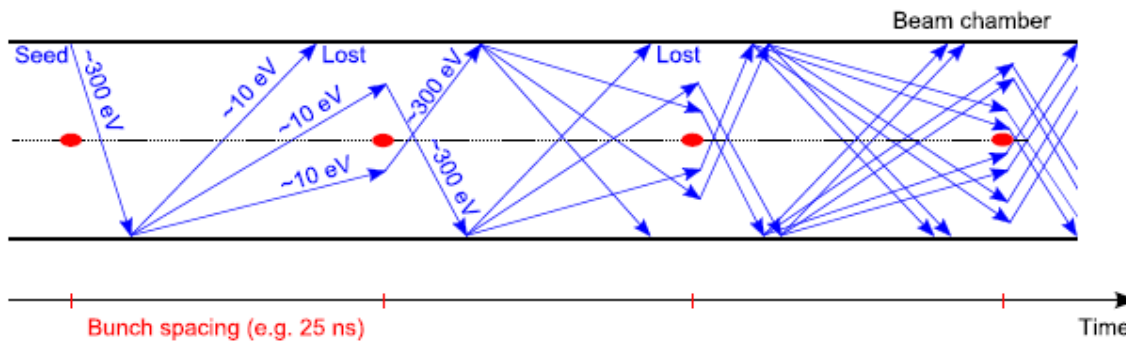
- The achievable luminosity critically depends on the geometry of the storage cell:
 $L \propto D^{-3} \Rightarrow$ **smaller diameter** \Leftrightarrow **higher luminosity**
- The cell aperture (diameter) must comply with the beam size in the stability region (dynamic aperture)



A storage cell with $R = 0.5$ cm has still a good safe factor for the machine aperture.

2. Electron clouds and surface coating

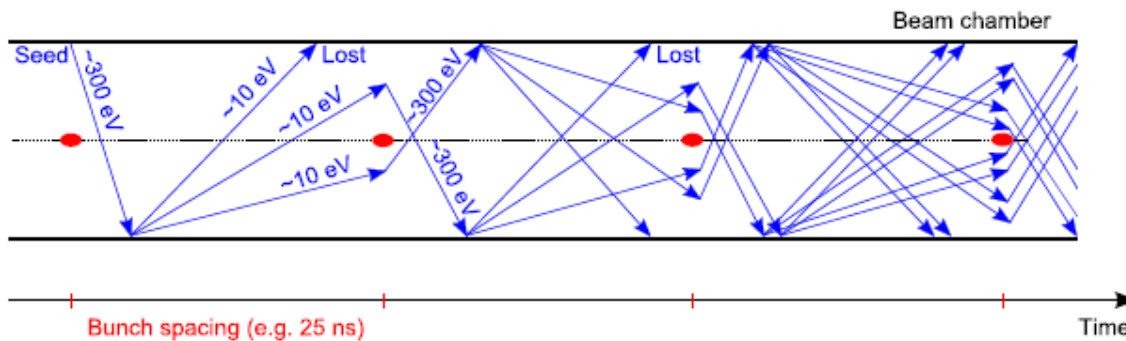
Slow electrons produced by various ionization processes are trapped near the beam and accelerated by the bunches, producing Secondary Electrons which may lead to an avalanche multiplication effect, forming dense **Electron Clouds** ...as a result, **transverse instabilities of the beam** may occur!



Surfaces close to the beam must have **low Secondary Emission Yield (SEY)**.

2. Electron clouds and surface coating

Slow electrons produced by various ionization processes are trapped near the beam and accelerated by the bunches, producing Secondary Electrons which may lead to an avalanche multiplication effect, forming dense **Electron Clouds** ...as a result, **transverse instabilities of the beam** may occur!

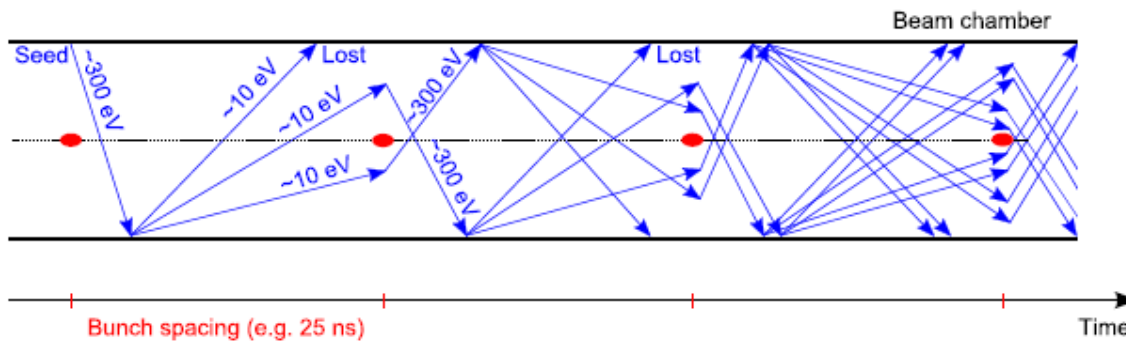


Surfaces close to the beam must have **low Secondary Emission Yield (SEY)**.

- As for SMOG2, **amorphous Carbon** turns out to be an efficient solution for the PGT
- Recent studies indicate good performances of a-C in preventing atomic recombination (\rightarrow loss of polarization).
- No need to generate an ice layer on the cell walls (HERMES)
- Amorphous graphite is already applied in accelerators, incl. SPS and LHC.

2. Electron clouds and surface coating

Slow electrons produced by various ionization processes are trapped near the beam and accelerated by the bunches, producing Secondary Electrons which may lead to an avalanche multiplication effect, forming dense **Electron Clouds** ...as a result, **transverse instabilities of the beam** may occur!



Surfaces close to the beam must have **low Secondary Emission Yield (SEY)**.

- As for SMOG2, **amorphous Carbon** turns out to be an efficient solution for the PGT
- Recent studies indicate good performances of a-C in preventing atomic recombination (\rightarrow loss of polarization).
- No need to generate an ice layer on the cell walls (HERMES)
- Amorphous graphite is already applied in accelerators, incl. SPS and LHC.

ARYA

SurfAce and mateRial studies for Accelerator Technology And related topics
2.1.3 WP3. LHCspin: surface properties validation
(Responsible: Pasquale Di Nezza & Roberto Cimino, INFN-LNF and CERN)

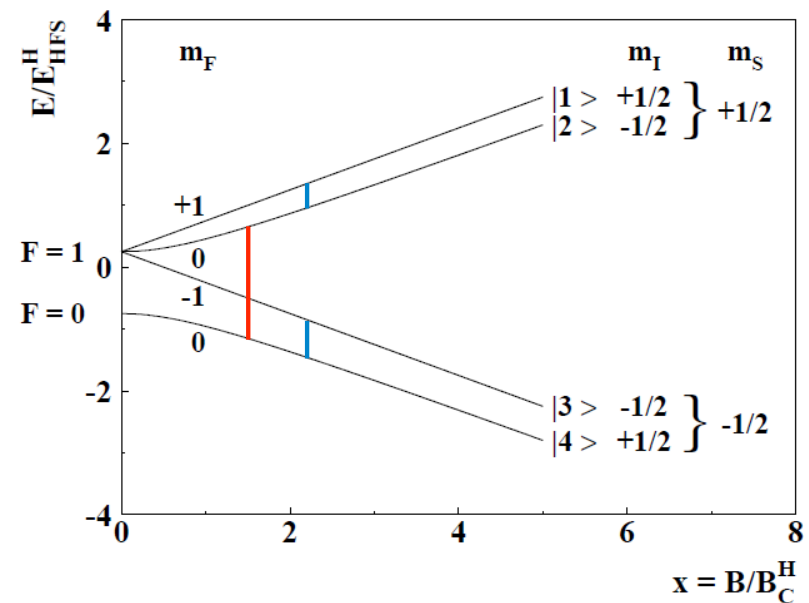


INFN dedicated program
for coating studies

+ a dedicated testbench for
coating studies in Juelich

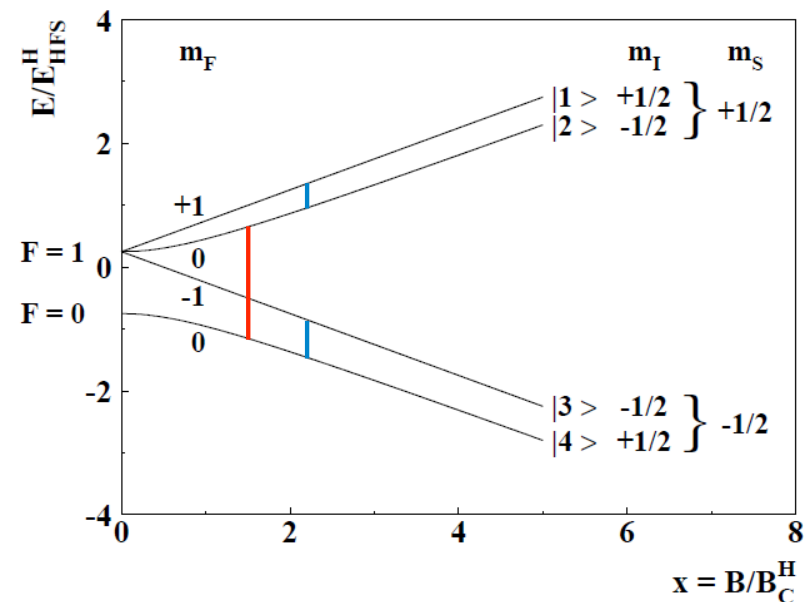
3. Beam-induced depolarization

- Consists in resonant transitions caused by the periodicity of the beam bunch field acting on the polarized H-atoms in an external magnetic field
- For transverse field, like at LHCspin, particularly critical is the **resonant σ_{2-4} transition**.



3. Beam-induced depolarization

- Consists in resonant transitions caused by the periodicity of the beam bunch field acting on the polarized H-atoms in an external magnetic field
- For transverse field, like at LHCspin, particularly critical is the **resonant σ_{2-4} transition**.

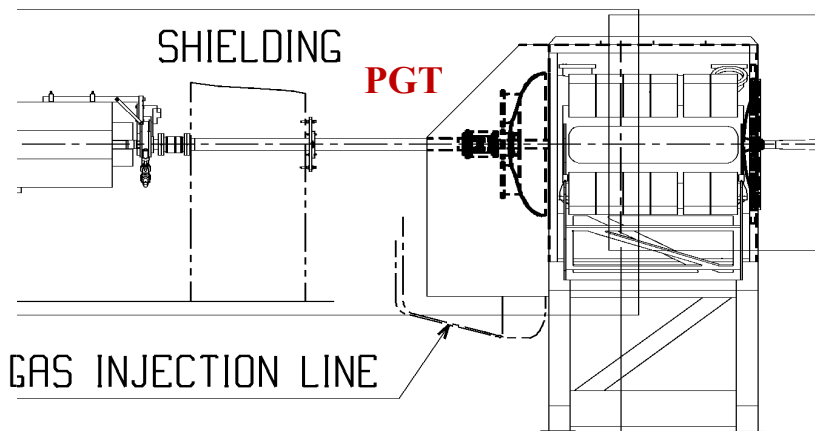


- LHC/HERA comparative studies (CERN-PBC-Notes-2018-001) have shown that **resonant depolarization** at the LHC via the σ_{2-4} transition is negligible compared to HERA, despite the 25x higher beam current!
- In order to further suppress the σ_{2-4} resonances, a **very high magnetic-field homogeneity** is mandatory → **strong requirement for the PGT transverse magnet**

Preliminary design studies

A new design for a compact polarized gas target

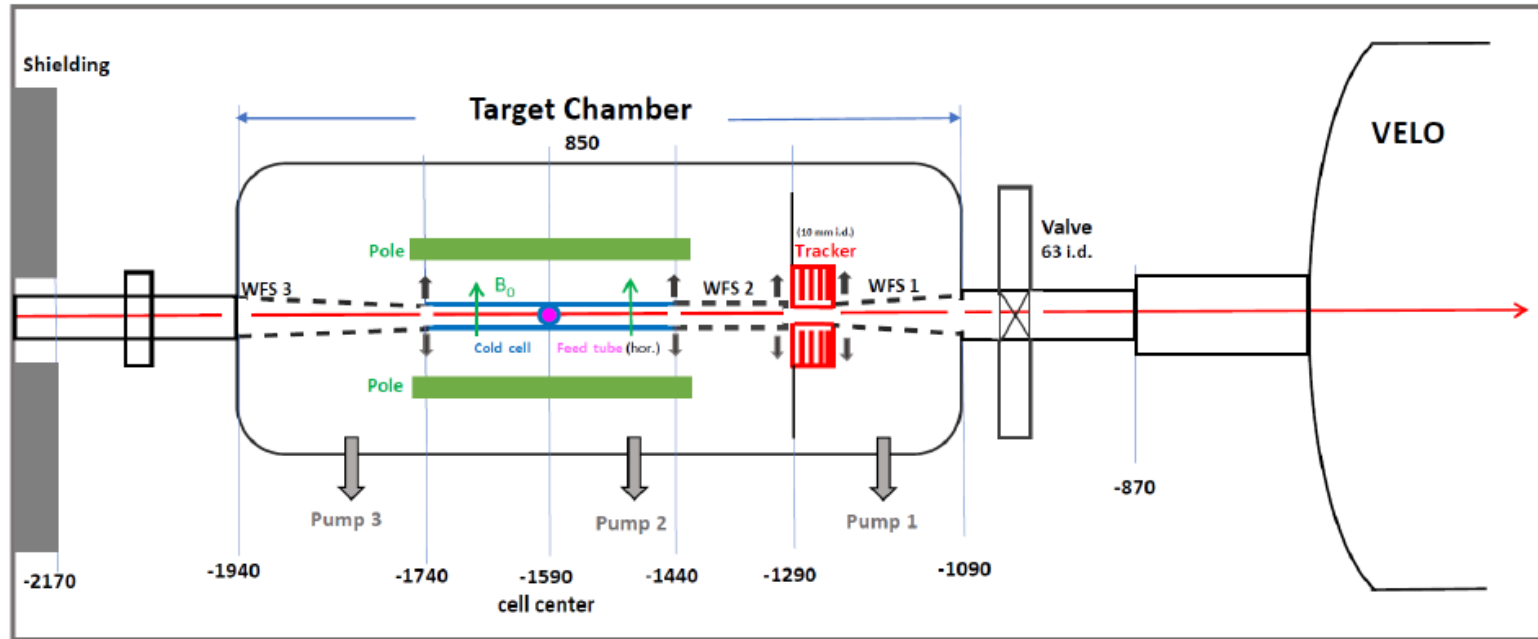
Space available in front of LHCb (~ 1.2 m)



Possible solutions:

1. Develop a compact ABS+diagnostic
2. Move the shielding wall upstream

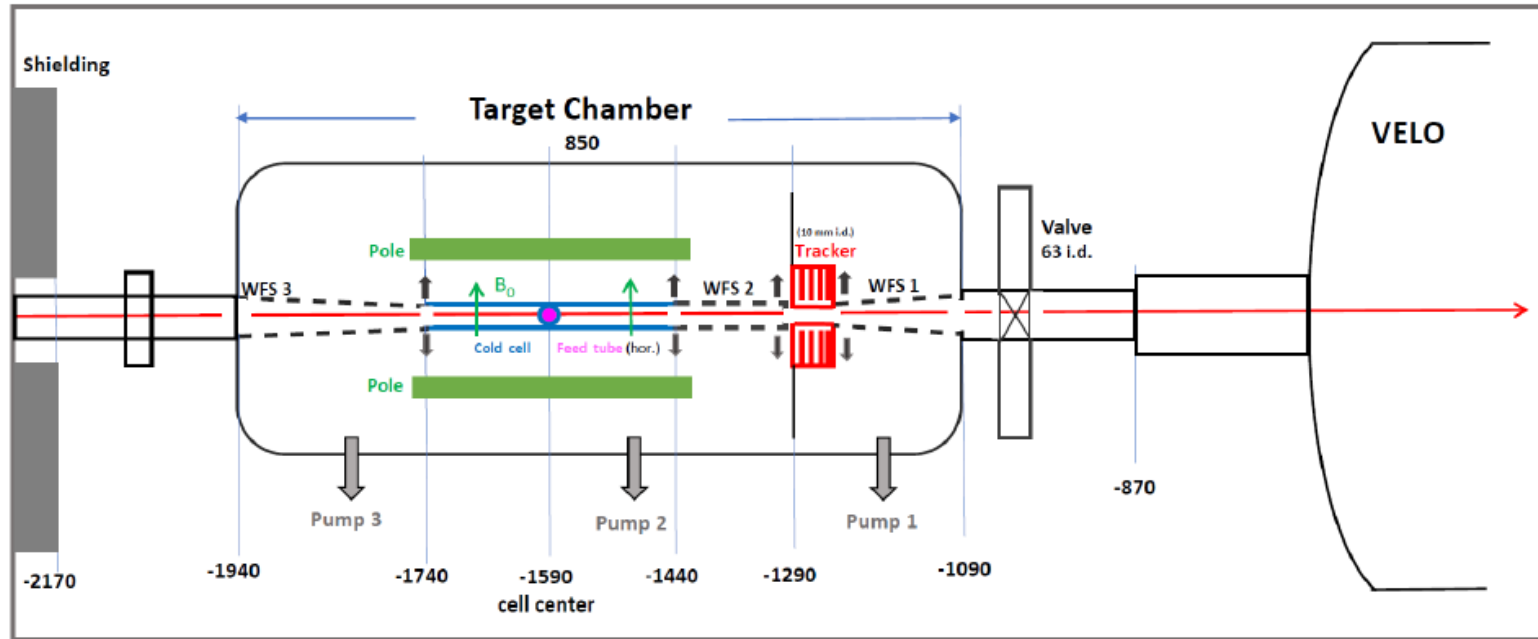
A new design for a compact polarized gas target



Beam line upstream of VELO:

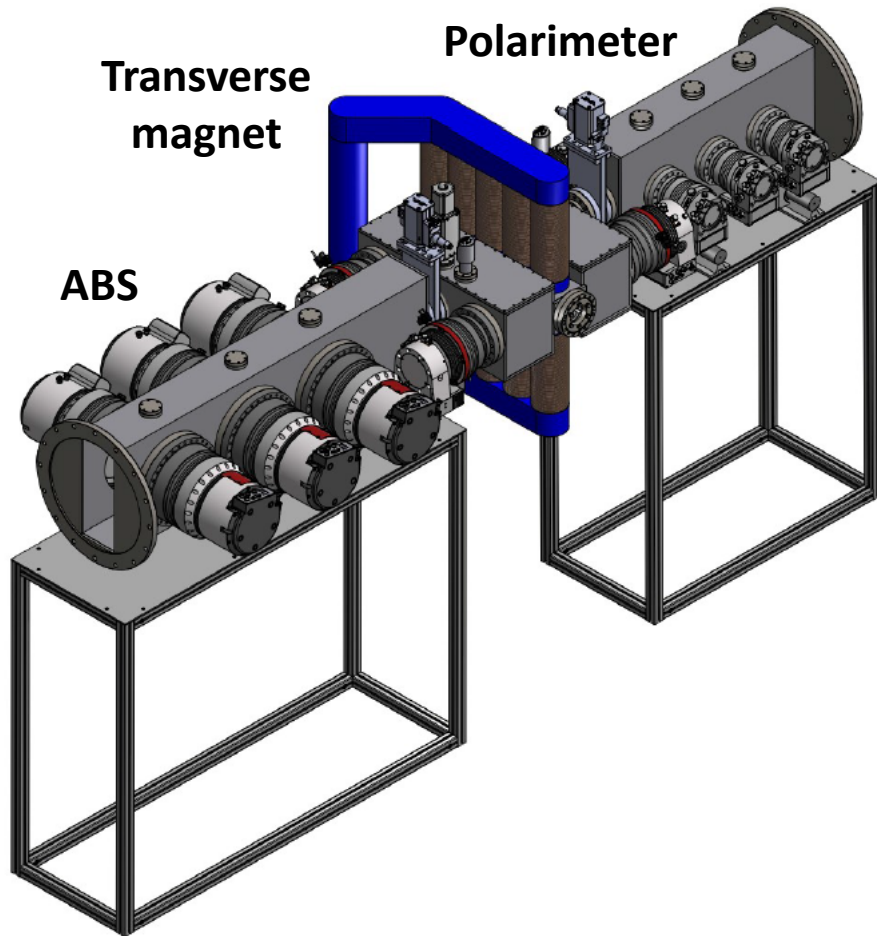
- Target Chamber
- Cell with beam tube (300 mm long)
- Gridded tube WFS 2 for differential pumping (200 mm)
- Tracker with 10 mm-opening
- Conical wake-field suppressors WFS 1 + 3.
- New sector valve (installed in LS2) and the entrance region of the VELO vessel.
- Upstream beam tube and shielding.

A new design for a compact polarized gas target

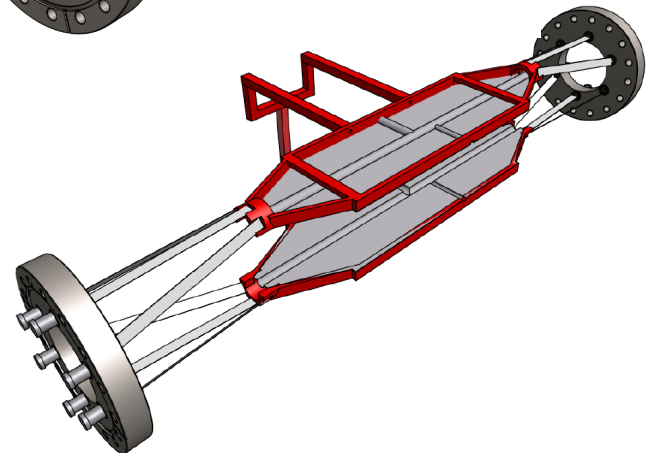
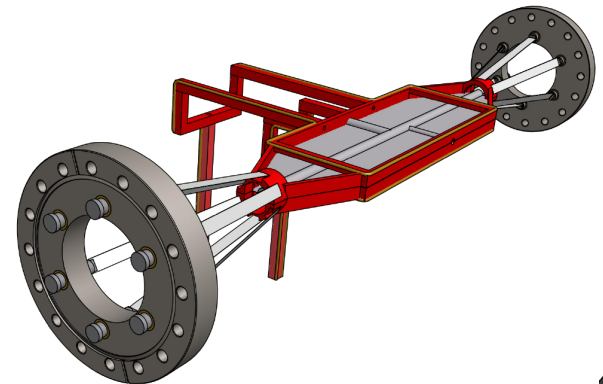
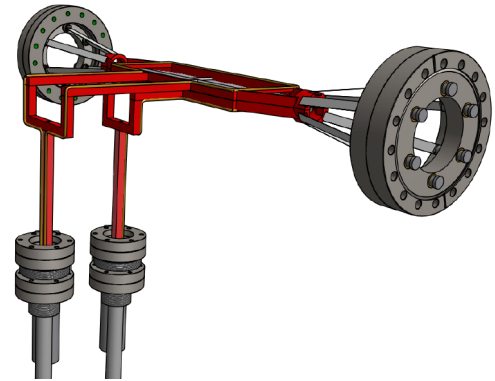
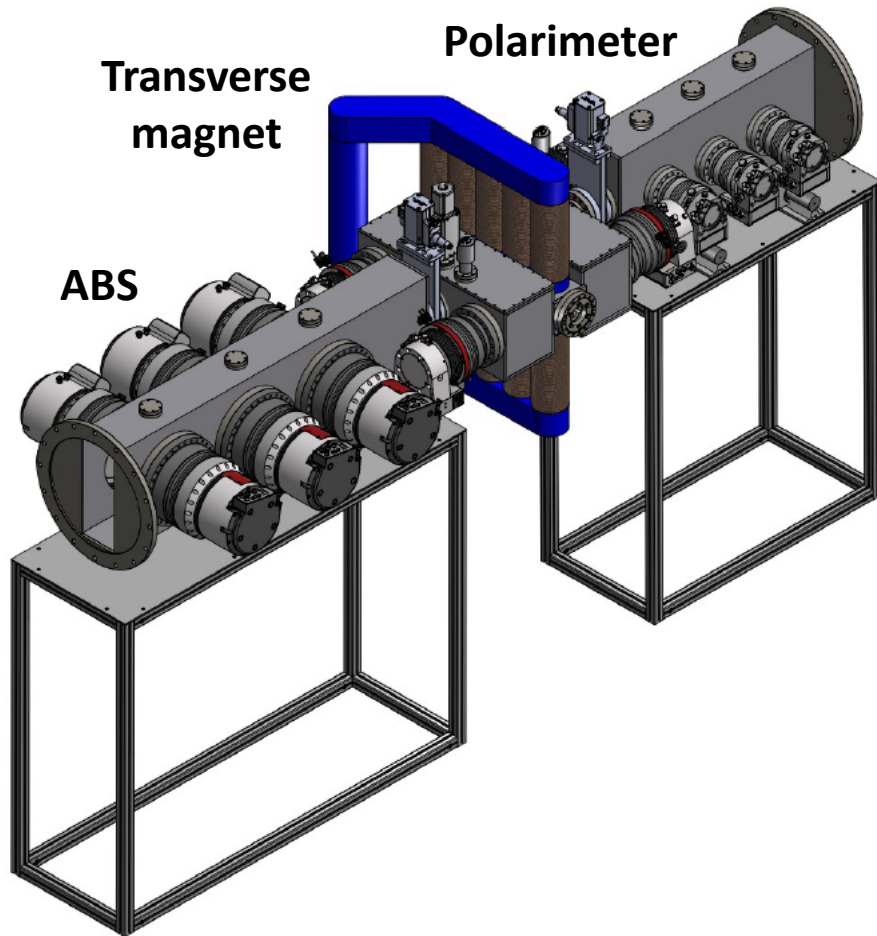


- The PGT can not be located close to or even inside the VELO vessel because of the **relatively high gas flow** which requires **differential pumping** on a separate target chamber
- Analytic estimates show that only 3% of downstream gas flow passes the 10 mm opening in the Tracker, 350 mm from cell center. This corresponds to $< 10^{-6}$ mb l/s flow rate of recombined H, i.e. **well within the tolerable range**.
- **MolFlow simulations** planned (including pumping by NEG coating)

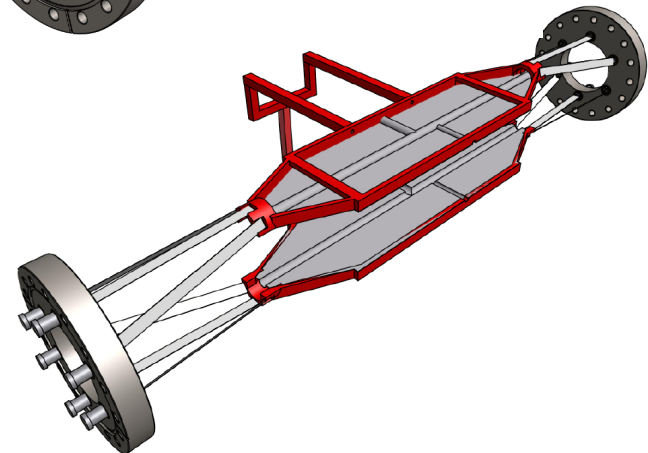
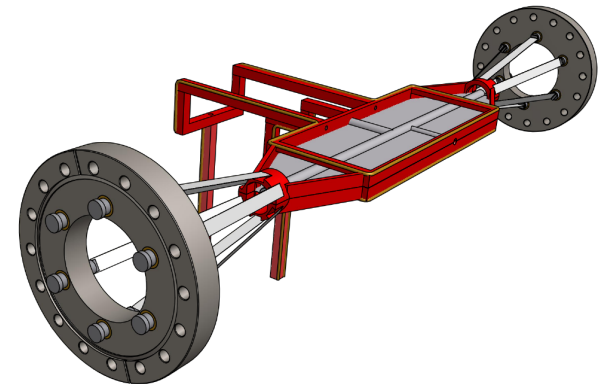
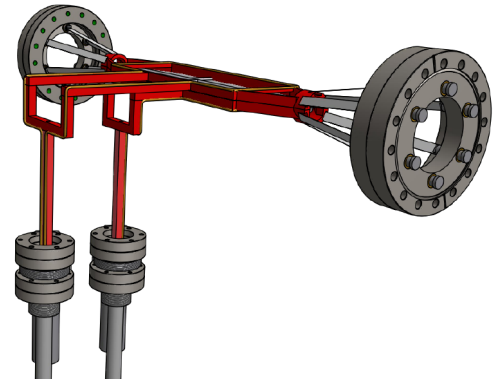
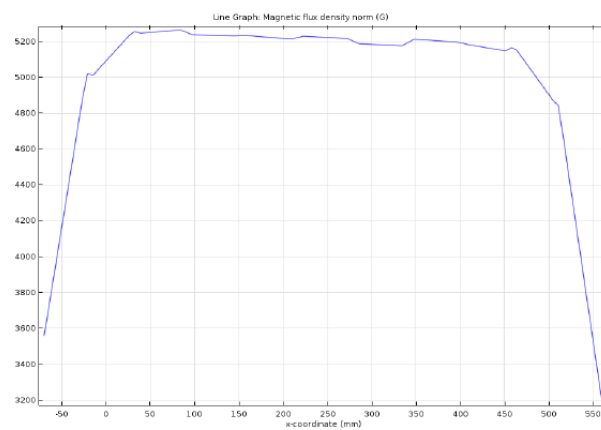
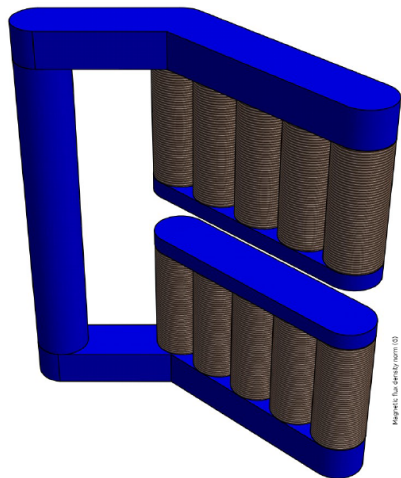
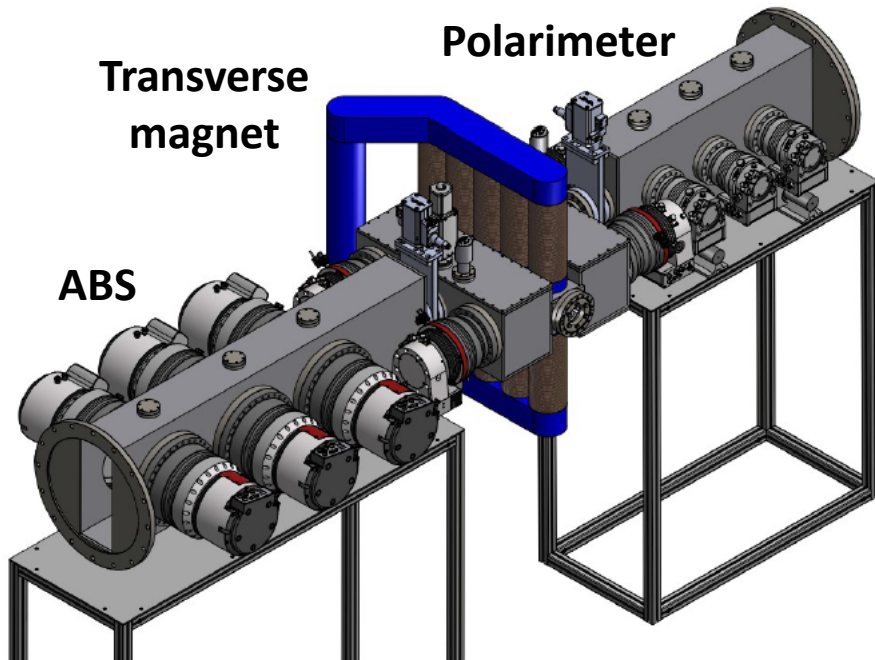
A new design for a compact polarized gas target



A new design for a compact polarized gas target



A new design for a compact polarized gas target



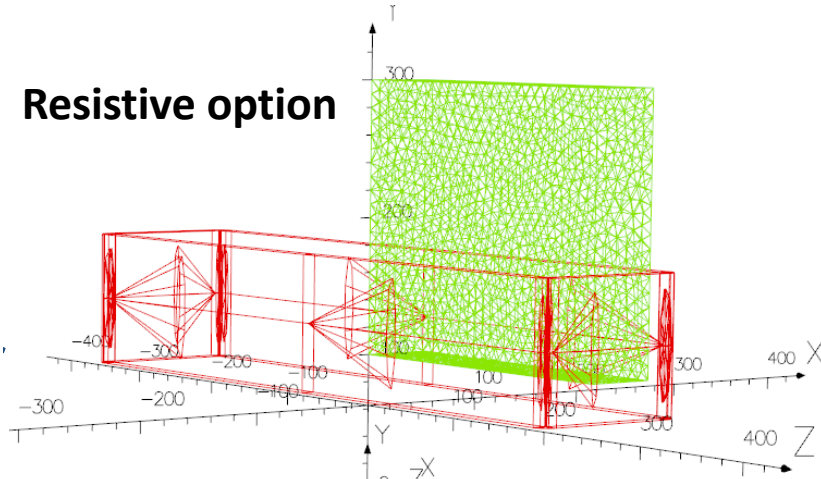
Other magnet options



Transverse magnetic Field 0.3 T

Field homogeneity: <5% over cell volume (300 mm long for 10 mm diam cell)

Resistive option



Pro: • Simple and standard

Cons: • water cooling required
• High voltage power converter
• 150 mm wide iron → bulky (heavy)

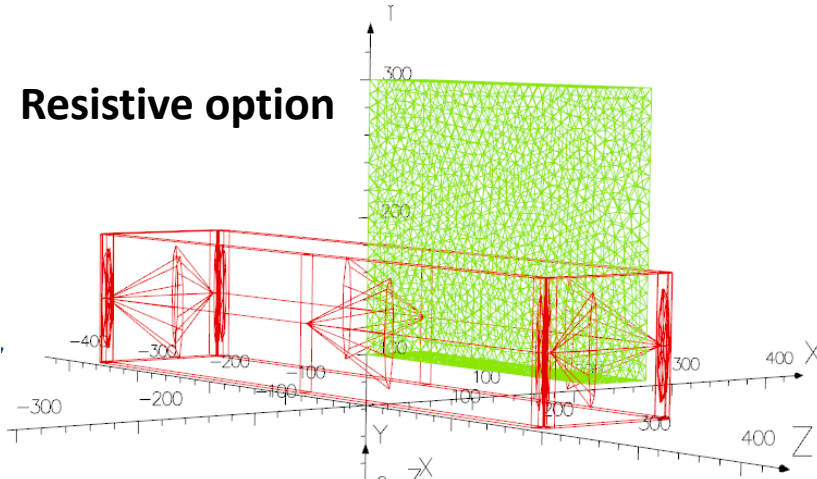
Other magnet options



Transverse magnetic Field 0.3 T

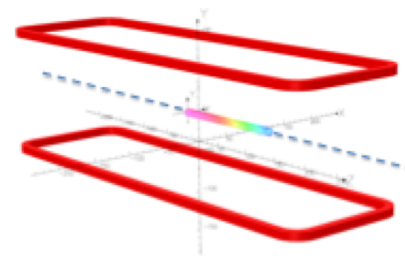
Field homogeneity: <5% over cell volume (300 mm long for 10 mm diam cell)

Resistive option

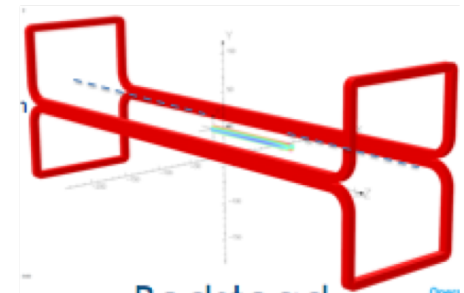


- Pro:** • Simple and standard
- Cons:** • water cooling required
• High voltage power converter
• 150 mm wide iron → bulky (heavy)

Superconductive options



Racetrack



Bedstead

- Pro:** • smaller volume
• low voltage power converters
- Cons:** • cryogenics
• quench protection

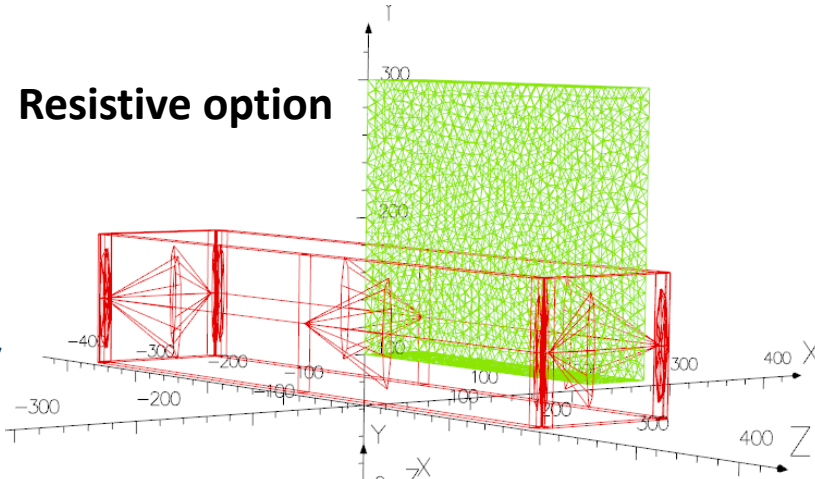
Other magnet options



Transverse magnetic Field 0.3 T

Field homogeneity: <5% over cell volume (300 mm long for 10 mm diam cell)

Resistive option

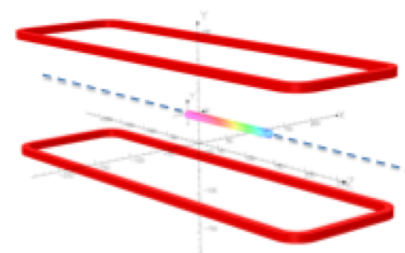


- Pro:**
- Simple and standard
- Cons:**
- water cooling required
 - High voltage power converter
 - 150 mm wide iron → bulky (heavy)

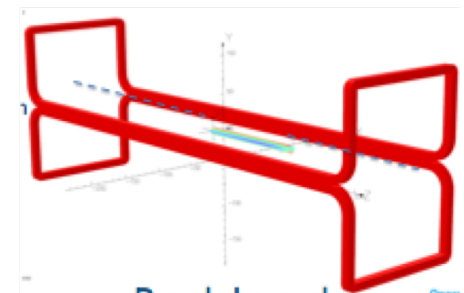
An interesting and fancy option (Canted cosine theta):

- | | |
|---------------------|-----------------------|
| Pro: | Cons: |
| • easy to wind | • field homogeneity ? |
| • easy to assembly | |
| • suitable for HTS? | |

Superconductive options

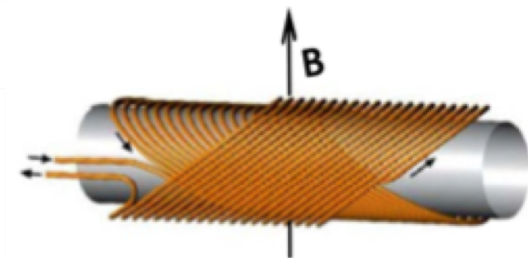


Racetrack



Bedstead

- Pro:**
- smaller volume
 - low voltage power converters
- Cons:**
- cryogenics
 - quench protection



Expected performances

Expected performances: target areal density



The LHC beam runs through the target cell and experiences an **average areal density**:

$$\theta = \frac{1}{2} \rho L \quad \left[\frac{\text{atoms}}{\text{cm}^2} \right] \quad \rho = \frac{I_0}{C_{\text{cell}}} \quad \left[\frac{\text{atoms}}{\text{cm}^3} \right]$$

$$I_0 = 6.5 \cdot 10^{16} \quad \left[\frac{\text{atoms}}{\text{s}} \right] \quad \text{intensity of pol. beam (HERMES ABS)}$$

$$C = 3.81 \sqrt{\frac{T(K)}{M}} \frac{D^3}{L + 1.33D} \quad \left[\frac{\text{l}}{\text{s}} \right] \quad \text{gas conductance through a tube section}$$

Expected performances: target areal density



The LHC beam runs through the target cell and experiences an **average areal density**:

$$\theta = \frac{1}{2} \rho L \left[\frac{\text{atoms}}{\text{cm}^2} \right] \quad \rho = \frac{I_0}{C_{\text{cell}}} \left[\frac{\text{atoms}}{\text{cm}^3} \right]$$

$$I_0 = 6.5 \cdot 10^{16} \left[\frac{\text{atoms}}{\text{s}} \right] \quad \text{intensity of pol. beam (HERMES ABS)}$$

$$C = 3.81 \sqrt{\frac{T(K)}{M}} \frac{D^3}{L + 1.33D} \left[\frac{\text{l}}{\text{s}} \right] \quad \text{gas conductance through a tube section}$$

Gas type	Areal density ($\times 10^{14}$) [atoms/cm ²]
H^\uparrow (300 K)	0.7
D^\uparrow (300 K)	1.0
H^\uparrow (100 K)	1.2
D^\uparrow (100 K)	1.7

■ Most probable scenario

■ Best case scenario ($\times \sqrt{3}$)

Expected performances: instantaneous luminosity



Two LHC beam intensity scenarios for Run4:

- **Conservative:** $I_{beam} = 3.63 \cdot 10^{18}$ prot/s ($N_{p/b} = 1.15 \times 10^{11}$, $N_b = 2808$)
- **Realistic:** $I_{beam} = 6.83 \cdot 10^{18}$ prot/s ($N_{p/b} = 2.2 \times 10^{11}$, $N_b = 2760$)

Expected performances: instantaneous luminosity



Two LHC beam intensity scenarios for Run4:

- **Conservative:** $I_{beam} = 3.63 \cdot 10^{18}$ prot/s ($N_{p/b} = 1.15 \times 10^{11}$, $N_b = 2808$)
- **Realistic:** $I_{beam} = 6.83 \cdot 10^{18}$ prot/s ($N_{p/b} = 2.2 \times 10^{11}$, $N_b = 2760$)

Gas type	Lumi (conserv.) [$cm^{-2}s^{-1}$] ($\times 10^{32}$)	Lumi (real.) [$cm^{-2}s^{-1}$] ($\times 10^{32}$)
H^\uparrow (300 K)	2.5	4.8
D^\uparrow (300 K)	3.6	6.8
H^\uparrow (100 K)	4.4	8.3
D^\uparrow (100 K)	6.2	11.7

■ Most probable scenario ■ Best case scenario ■ Worst case scenario

Expected performances: **integrated luminosity**



Three data-taking scenarios (days/year):

- 10 d/y (only short dedicated runs, a-la SMOG)
- 30 d/y (1 full month of dedicated runs)
- 200 d/y (running in parallel with collider mode)

Expected performances: integrated luminosity



Three data-taking scenarios (days/year):

- 10 d/y (only short dedicated runs, a-la SMOG)
- 30 d/y (1 full month of dedicated runs)
- 200 d/y (running in parallel with collider mode)

Gas type	Int. Lumi (conserv.) [fb^{-1}]			Int. Lumi (real.) [fb^{-1}]		
	10 d/y	30 d/y	200 d/y	10 d/y	30 d/y	200 d/y
H^\uparrow (300 K)	0.2	0.7	4.4	0.4	1.2	8.3
D^\uparrow (300 K)	0.3	0.9	6.2	0.6	1.8	11.7
H^\uparrow (100 K)	0.4	1.1	7.6	0.7	2.1	14.3
D^\uparrow (100 K)	0.5	1.6	10.8	1.0	3.0	20.3

■ Most probable scenario ■ Best case scenario ■ Worst case scenario

Expected performances: impact on beam life-time



$$\tau_{loss} = \frac{N_{p/beam}}{R_{loss}} = \frac{N_{p/beam}}{L \cdot \sigma_{beam-gas}}$$

$$\sigma_{beam-gas} \sim A^{2/3} \sigma_{pp}$$

$$\sigma_{pp}(115 \text{ GeV}) \sim 50 \text{ mb}$$

Expected performances: impact on beam life-time



$$\tau_{loss} = \frac{N_{p/beam}}{R_{loss}} = \frac{N_{p/beam}}{L \cdot \sigma_{beam-gas}}$$

$$\sigma_{beam-gas} \sim A^{2/3} \sigma_{pp}$$

$$\sigma_{pp}(115 \text{ GeV}) \sim 50 \text{ mb}$$

Gas type	τ_{loss} (days)
H^{\uparrow} (300 K)	294
D^{\uparrow} (300 K)	131
H^{\uparrow} (100 K)	169
D^{\uparrow} (100 K)	75

■ Most probable scenario

■ Worst case scenario

The partial beam decay-time due solely to beam-gas collisions is negligible compared to the average duration of a fill (10 h).

Conclusions

- A fixed-target physics program is already ongoing at LHCb with SMOG
- **The proposed upgrade SMOG2 is now approved and in production phase. Installation completed by January 2020!**
- **The polarized target option is the natural evolution of SMOG2.** It is taken into serious consideration by the LHCb Collaboration and LHC machine experts! R&D is ongoing. Expected installation during LHC LS3 (2024-2026).

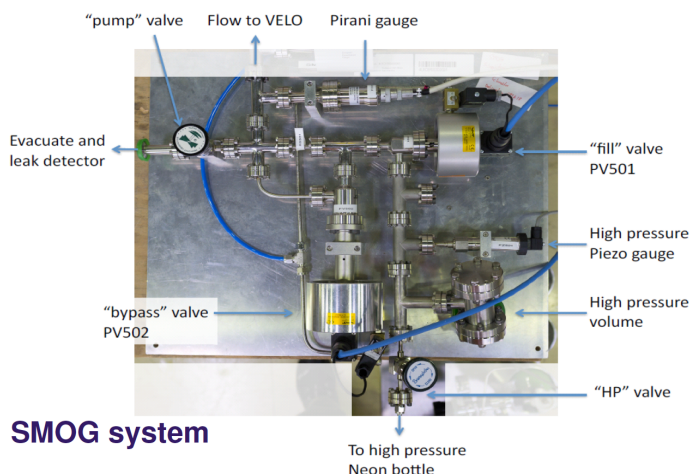
Conclusions

- A fixed-target physics program is already ongoing at LHCb with SMOG
- **The proposed upgrade SMOG2 is now approved and in production phase. Installation completed by January 2020!**
- **The polarized target option is the natural evolution of SMOG2.** It is taken into serious consideration by the LHCb Collaboration and LHC machine experts! R&D is ongoing. Expected installation during LHC LS3 (2024-2026).
- Many critical aspects of the project (aperture, coating, magnetic field, beam lifetime, impedance, space constraints, etc.) have to cope with the requirements from the machine and are being studied carefully.
- The expected performances are very promising and will allow, for the first time, for a rich and ambitious spin-physics program at LHC!

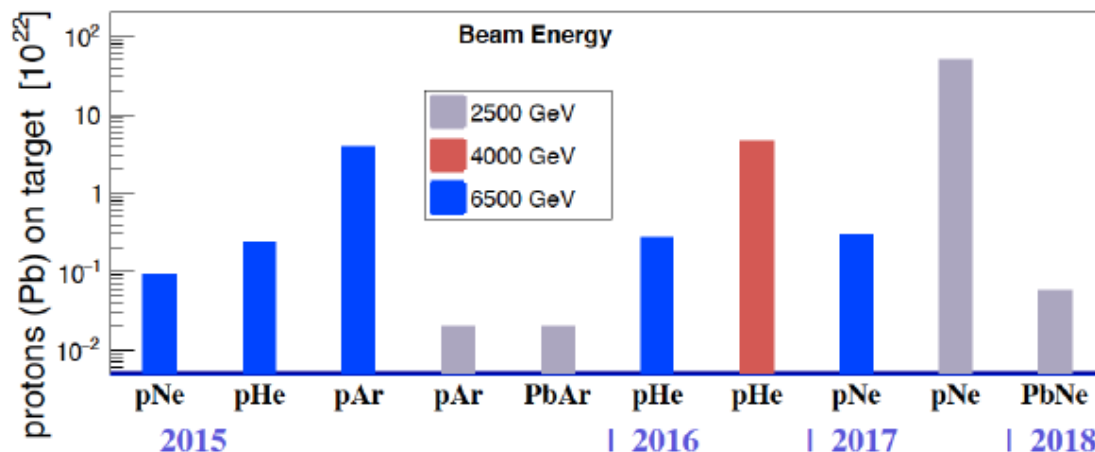
BACK-UP

The LHCb fixed-target system SMOG

The SMOG system gives the unique opportunity to operate an **LHC experiment in a fixed target mode** and to study pA and AA collisions on various targets!



SMOG system



Advantages of a fixed gaseous target:

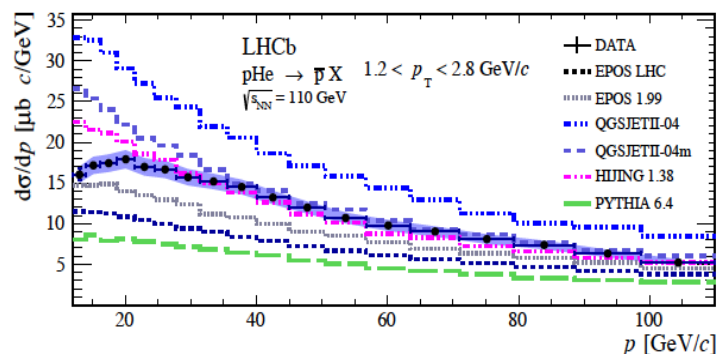
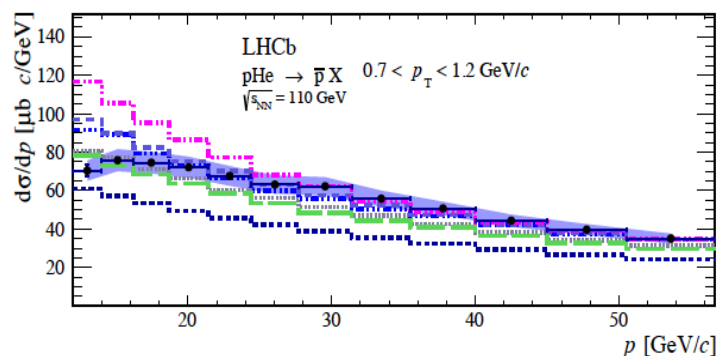
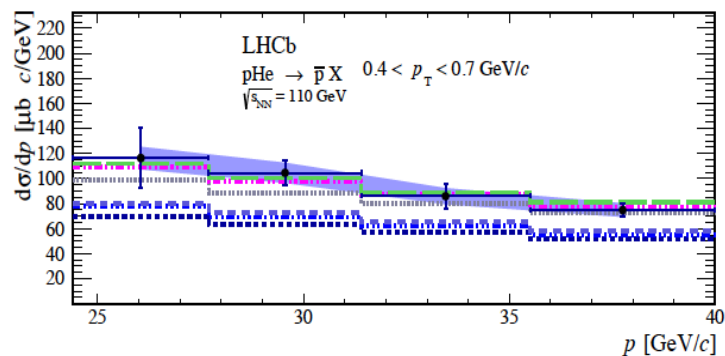
- ✓ **Unique kinematic conditions**
 - $\sqrt{s} \approx 110$ GeV
 - backward CM rapidity ($-3.0 \lesssim y_{CM} \lesssim 0$) sensitive to poorly explored high x -Bjorken
- ✓ **Marginal impact on LHC beam and mainstream physics at current experiments**
- ✓ **Measurement of charm production in pHe and pAr collisions** [Phys. Rev. Lett. 122, 132002 \(2019\)](#)
- ✓ **Measurement of antiproton production in pHe collisions** [Phys. Rev. Lett. 121, 222001 \(2018\)](#)

Largest sample: pNe ($L \sim 100$ nb $^{-1}$)

First physics results with SMOG

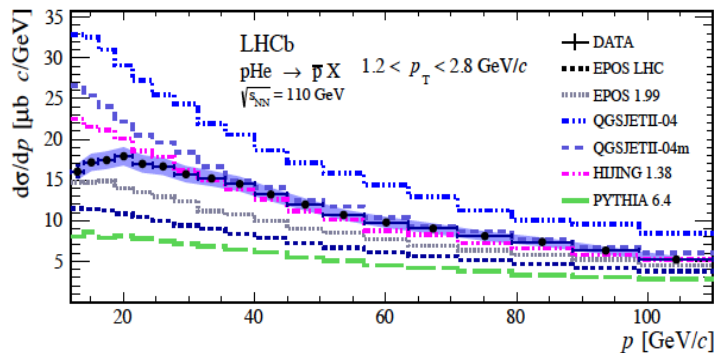
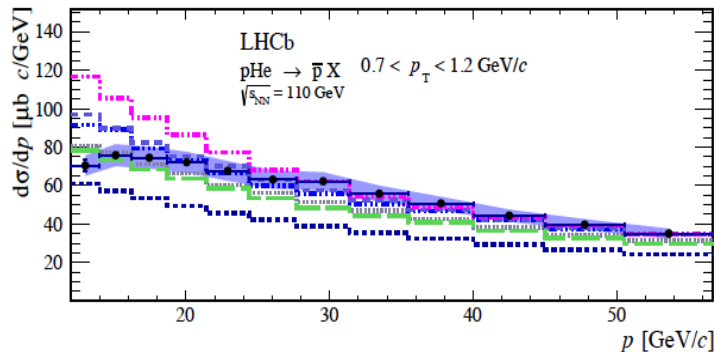
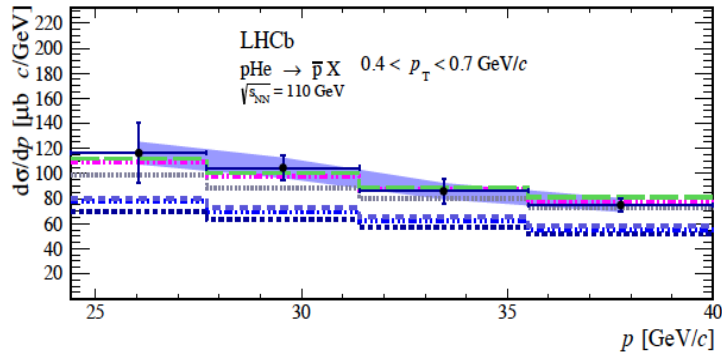
Antiproton production in p-He collisions

➤ First measurement of \bar{p} production in pHe collisions at $\sqrt{s_{NN}} = 110$ GeV [arXiv:1808.06127](https://arxiv.org/abs/1808.06127)

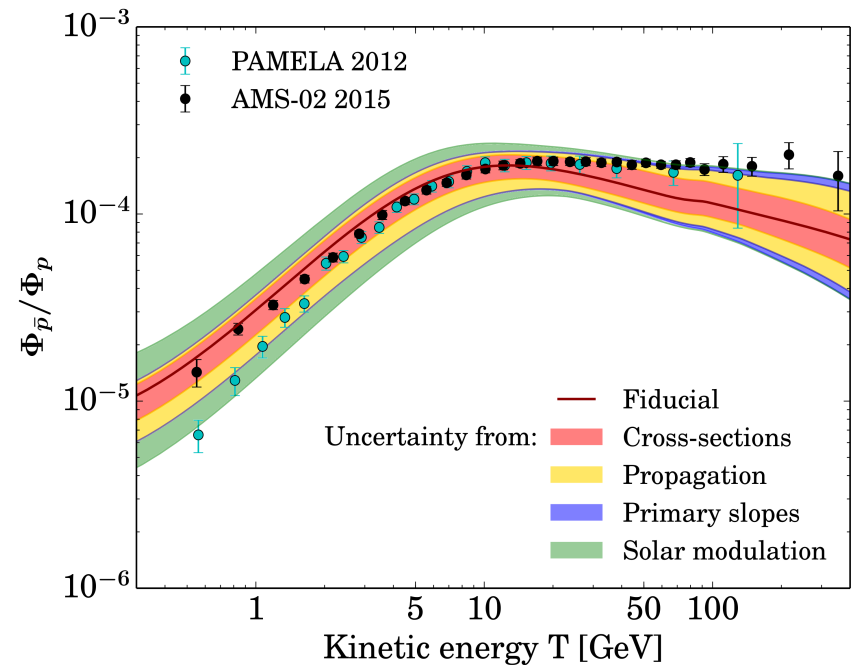


Antiproton production in p-He collisions

➤ First measurement of \bar{p} production in pHe collisions at $\sqrt{s_{NN}} = 110$ GeV [arXiv:1808.06127](https://arxiv.org/abs/1808.06127)

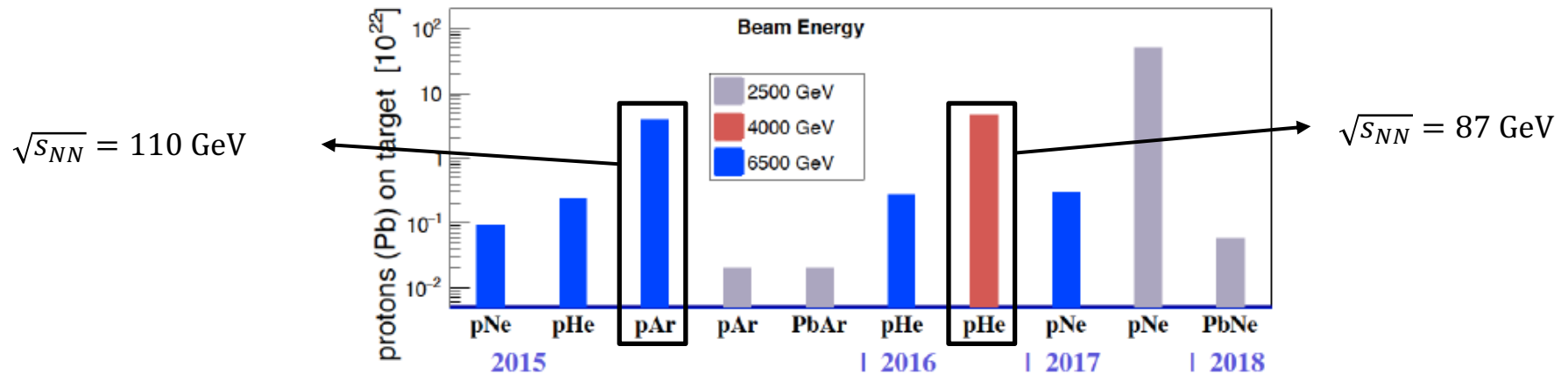


Relevant for cosmic-rays/DM physics: predictions for \bar{p}/p flux ratio from spallation of primary cosmic rays on interstellar medium (H and He) are presently limited by large uncertainties on \bar{p} production cross sections (especially from He)



Prompt charm production in p-He and p-Ar collisions

- First measurement of J/ψ and D^0 production in p-He ($\sqrt{s_{NN}} = 87$ GeV) and p-Ar ($\sqrt{s_{NN}} = 110$ GeV) collisions with SMOG.



Prompt charm production in p-He and p-Ar collisions

- **First measurement of J/ψ and D^0 production in p-He ($\sqrt{s_{NN}} = 87$ GeV) and p-Ar ($\sqrt{s_{NN}} = 110$ GeV) collisions with SMOG.**

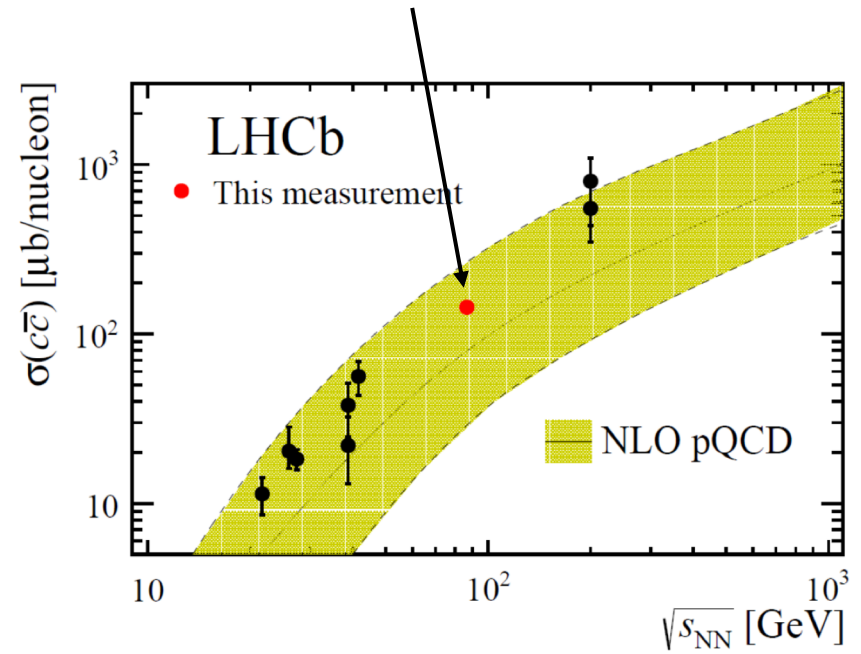
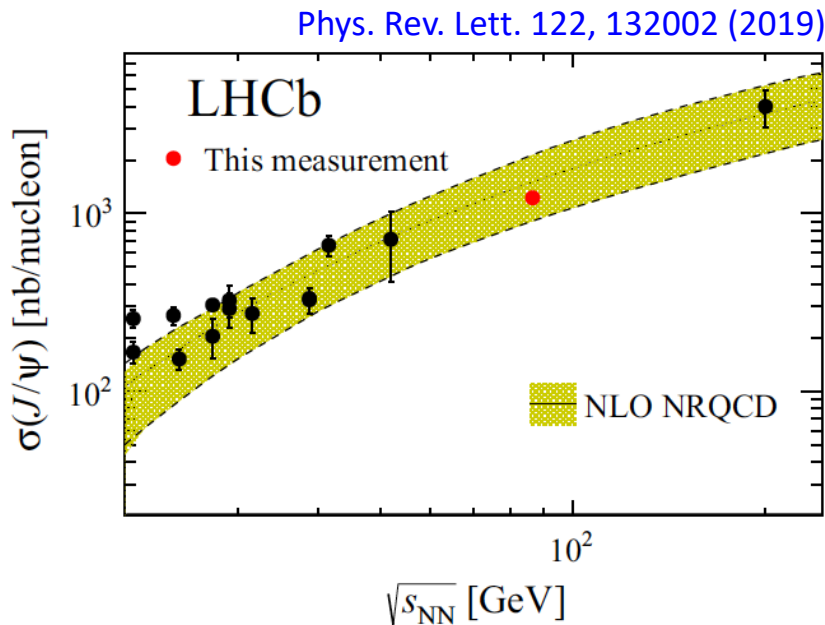
$$\sigma_{J/\psi} = 1225.6 \pm 100.7 \text{ nb/nucleon}$$

$$\sigma_{D^0} = 156.0 \pm 13.1 \text{ nb/nucleon}$$



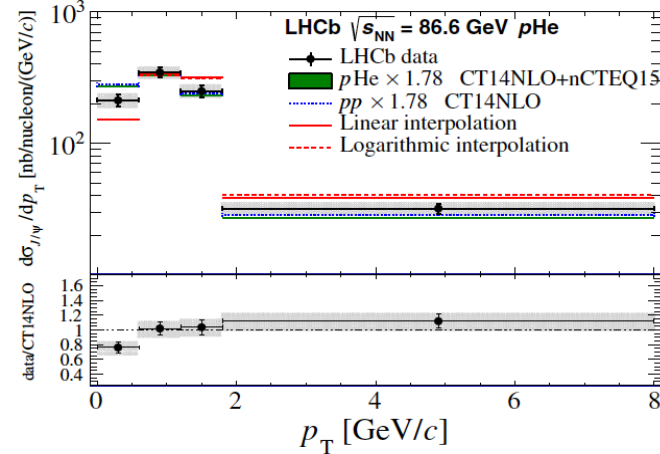
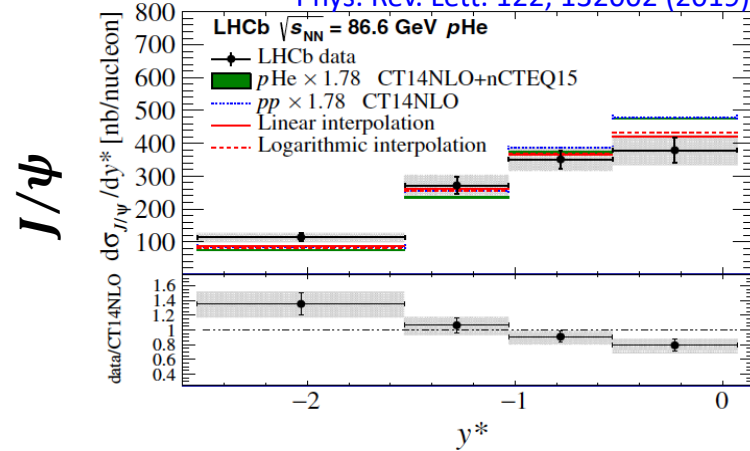
scaled with global $f(c \rightarrow D^0)$ FF to obtain the $c\bar{c}$ production cross section:

$$\sigma_{c\bar{c}} = 144.0 \pm 12.1 \pm 3.5 \text{ nb/nucleon}$$



Prompt charm production in p-He collisions at $\sqrt{s} = 87$ GeV

Phys. Rev. Lett. 122, 132002 (2019)

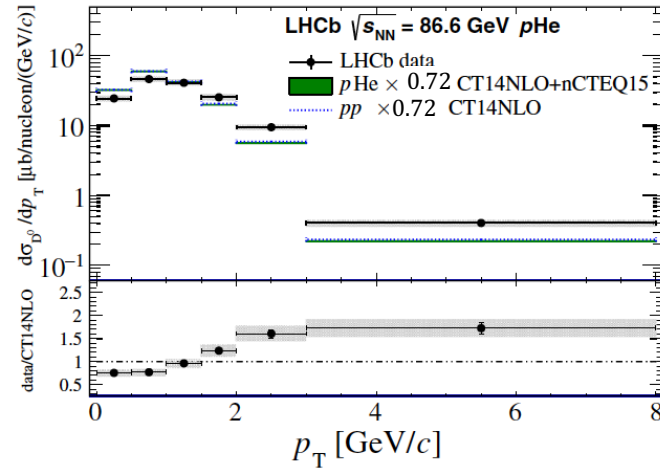
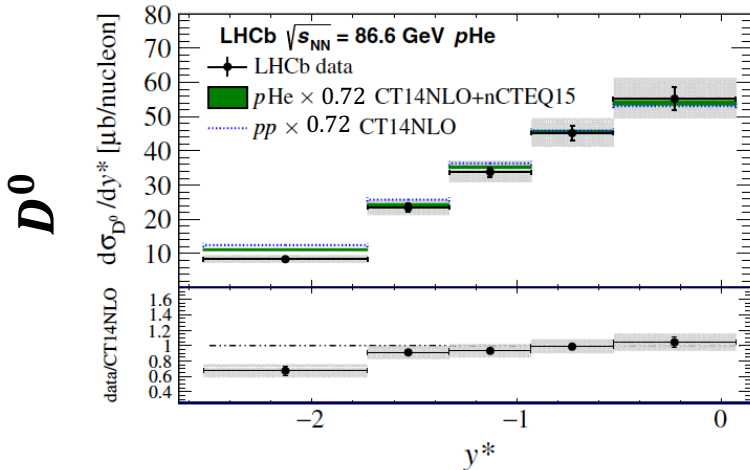


HELAC-ONIA predictions:

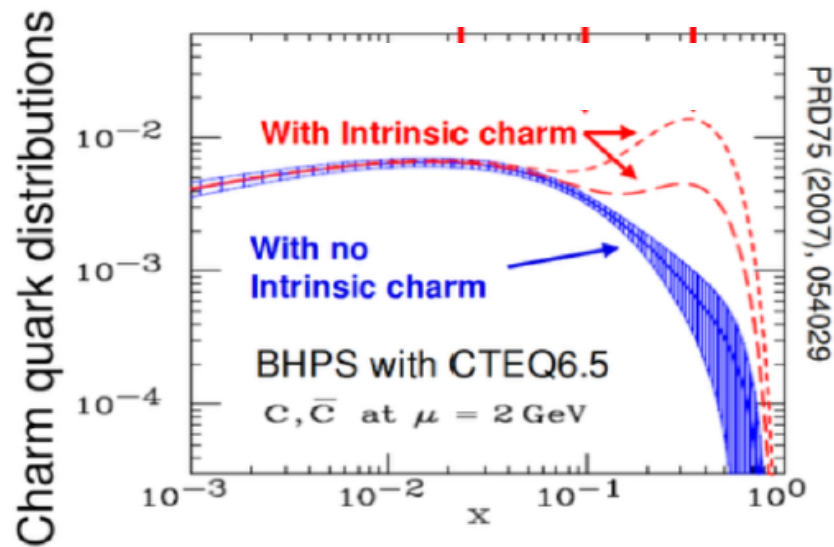
- JHEP 1303 (2013) 122
- Eur. Phys. J. C 77, 1 (2017)
- Comput. Phys. Commun. 198, 238 (2016)

Phenom. models:

- JHEP 1303 (2013) 122
- JHEP 05 (2013) 155

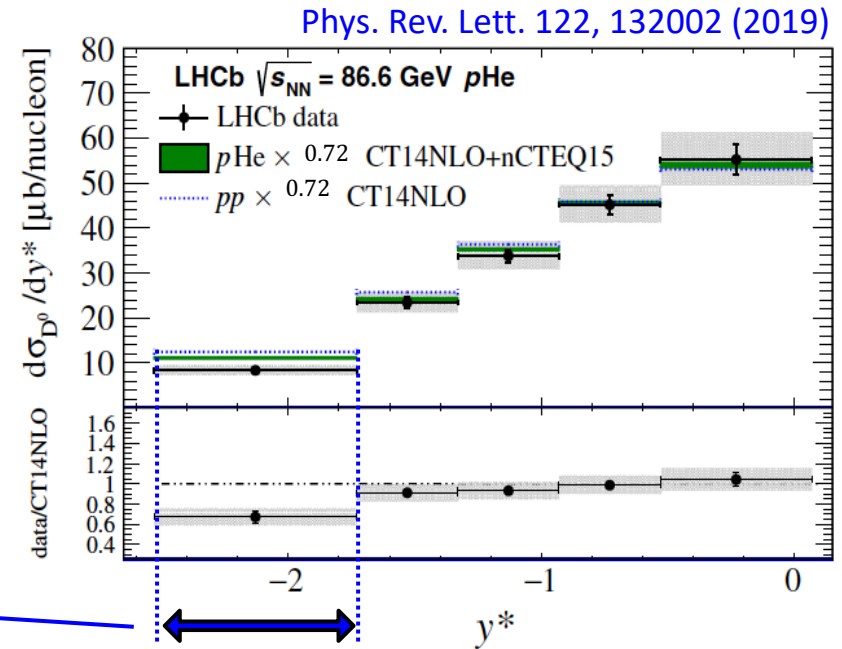
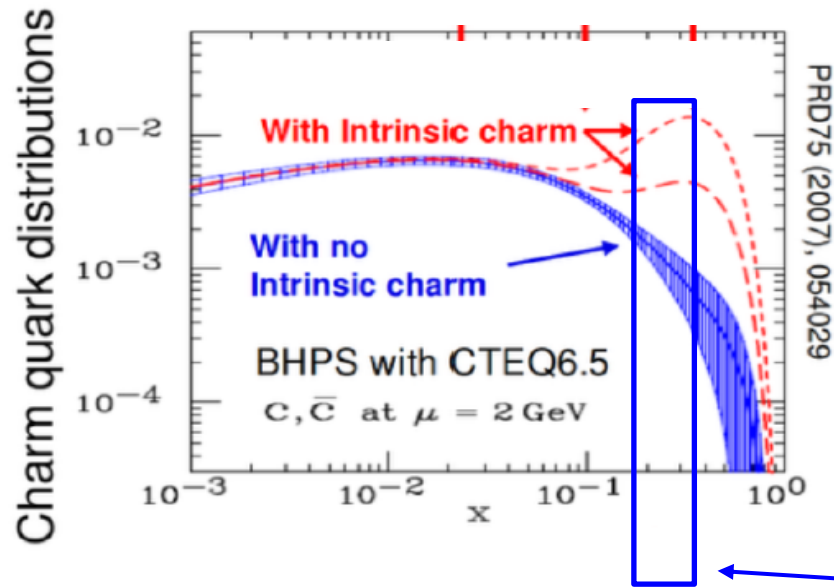


Do we observe effects from intrinsic charm?



- 5-quark Fock state of the proton may contribute at high x !

Do we observe effects from intrinsic charm?



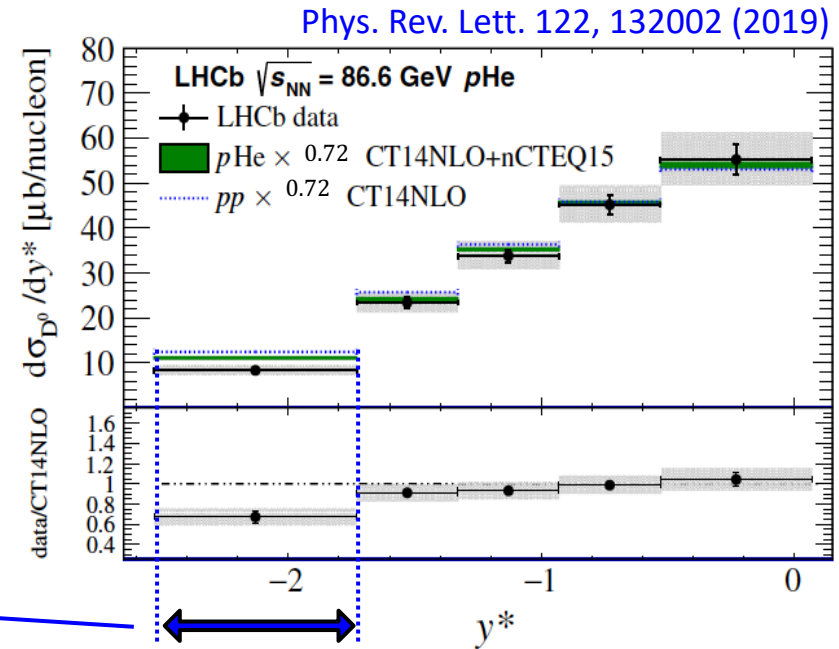
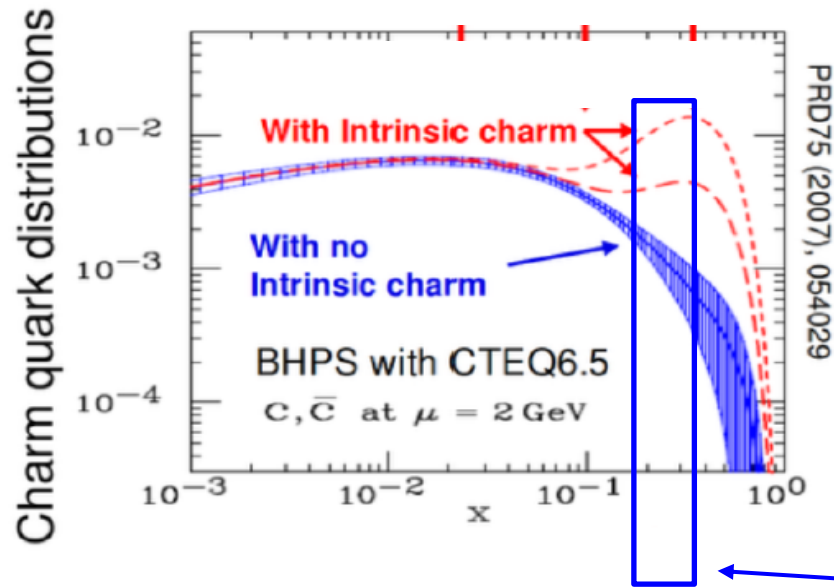
- 5-quark Fock state of the proton may contribute at high x !
- The most backward bin corresponds to $x \in [0.17, 0.37]$
- In this range intrinsic charm is expected to be large

$$x \simeq \frac{2m_c}{\sqrt{s_{NN}}} e^{-y^*}$$

$$\Downarrow$$

$$\text{high } x \leftrightarrow y^* < 0$$

Do we observe effects from intrinsic charm?



$$x \simeq \frac{2m_c}{\sqrt{s_{NN}}} e^{-y^*}$$

$$\Downarrow$$

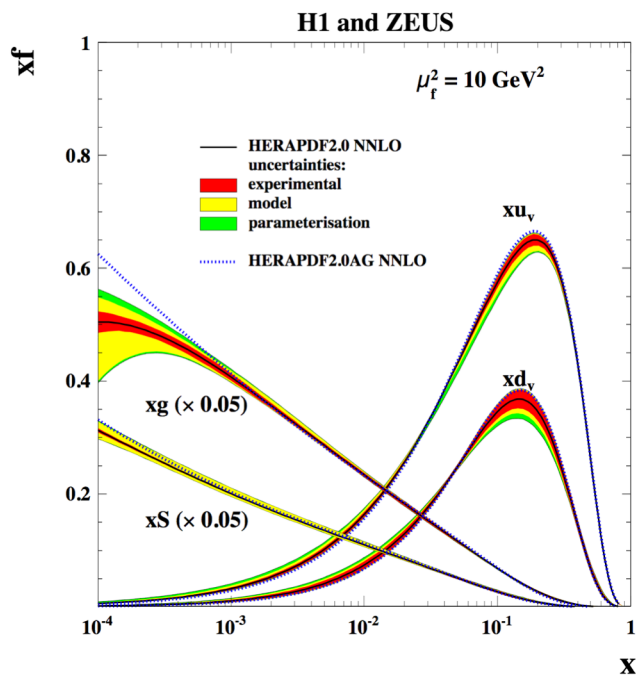
$$\text{high } x \leftrightarrow y^* < 0$$

- 5-quark Fock state of the proton may contribute at high x !
- The most backward bin corresponds to $x \in [0.17, 0.37]$
- In this range intrinsic charm is expected to be large
- No strong effect is seen by comparing data with theoretical prediction (which do not include any intrinsic charm contribution)

Studying the 3D structure of nucleons with fixed-target collisions at LHCb

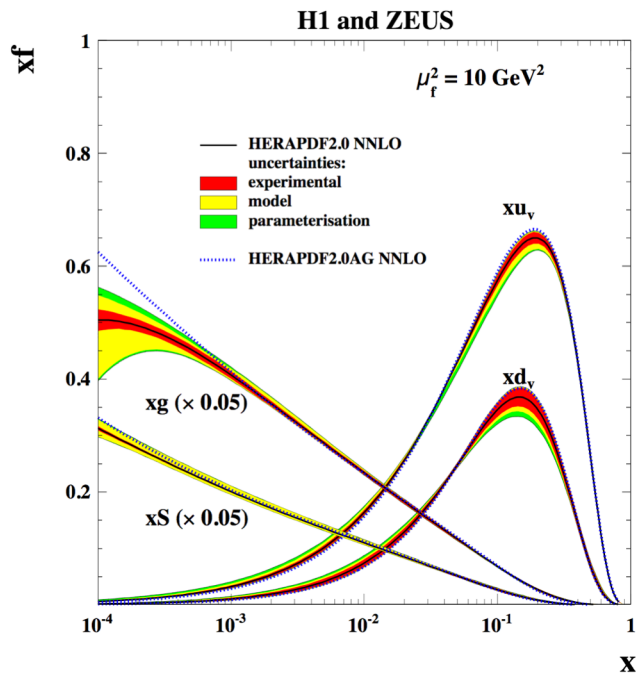
Accessing the nucleon structure

The present knowledge of the nucleon structure is dominated by **collinear (unpol.) PDFs**, measured with great precision in decades of DIS experiments

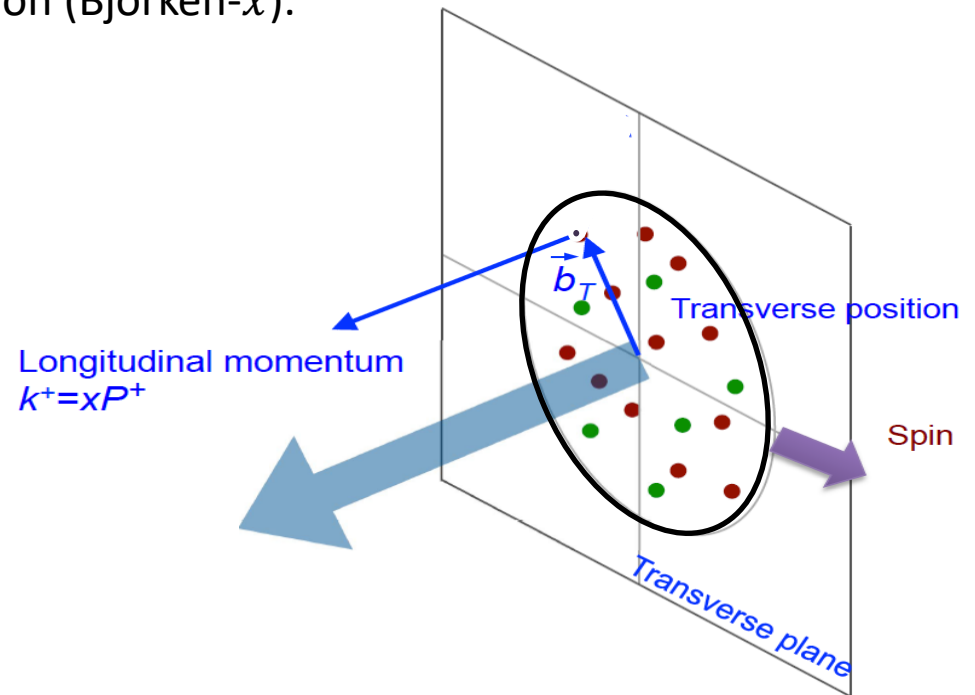


Accessing the nucleon structure

The present knowledge of the nucleon structure is dominated by **collinear (unpol.) PDFs**, measured with great precision in decades of DIS experiments

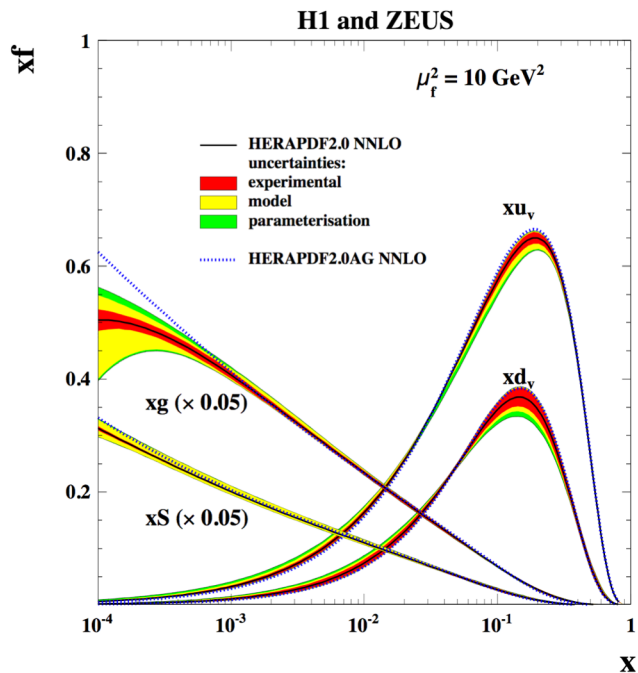


Despite the high level of accuracy, collinear PDFs provide only a 1-dim description of the nucleon structure, in terms of the parton long. momentum fraction (Bjorken- x).



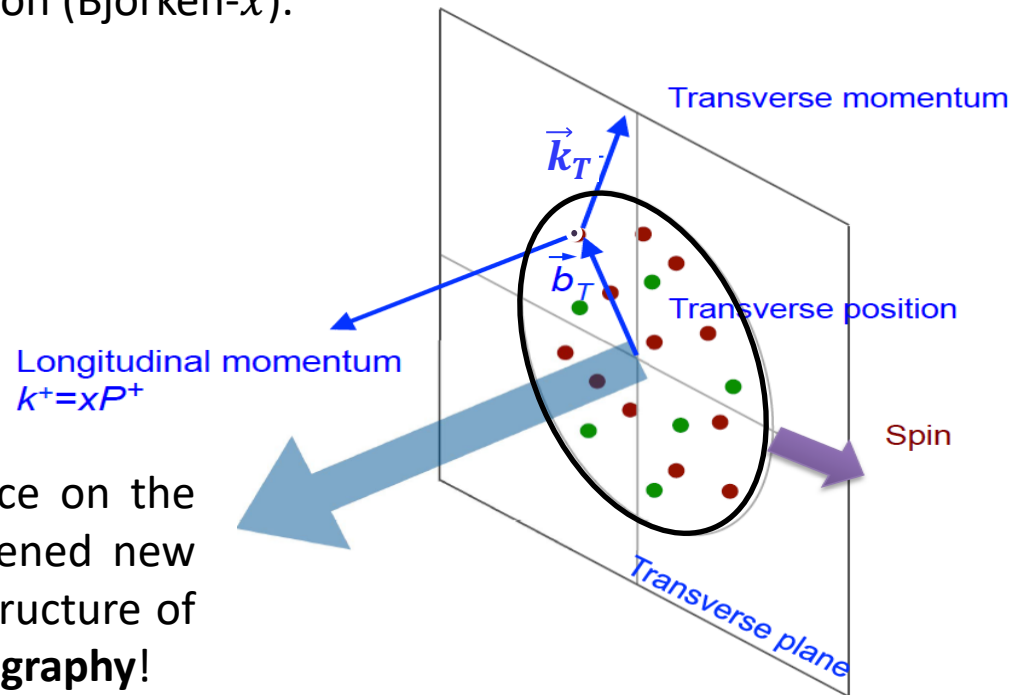
Accessing the nucleon structure

The present knowledge of the nucleon structure is dominated by **collinear (unpol.) PDFs**, measured with great precision in decades of DIS experiments



Despite the high level of accuracy, collinear PDFs provide only a 1-dim description of the nucleon structure, in terms of the parton long. momentum fraction (Bjorken- x).

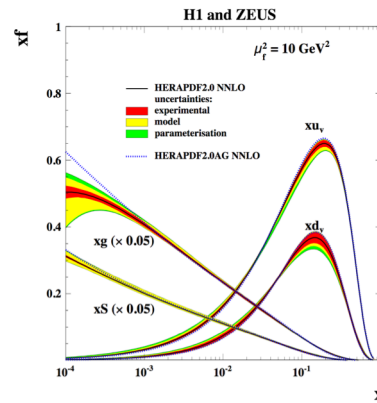
Considering also the explicit dependence on the parton transverse momenta k_T has opened new perspectives in the exploration of the structure of the nucleon! ...**TMD PDFs, nucleon tomography!**



Mapping the nucleon structure

Collinear PDFs

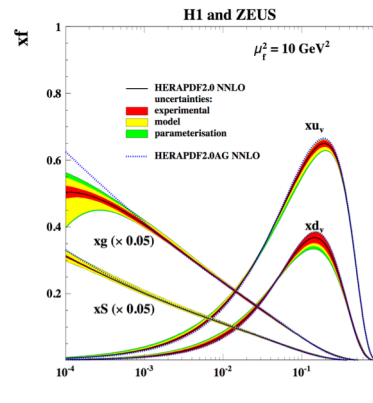
1D



Mapping the nucleon structure

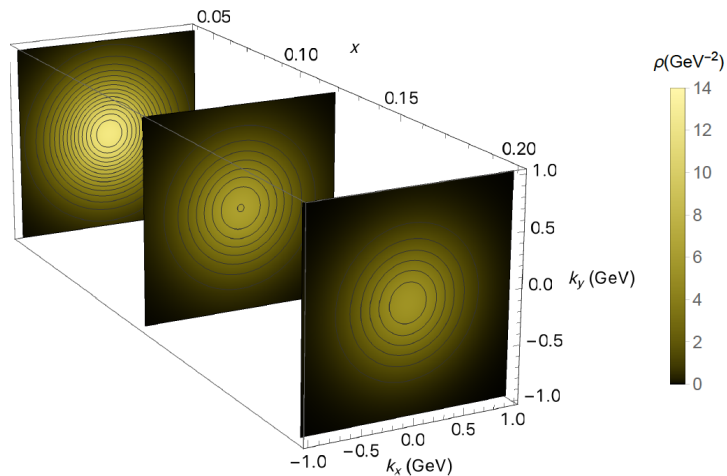
Collinear PDFs

1D



TMDs

3D

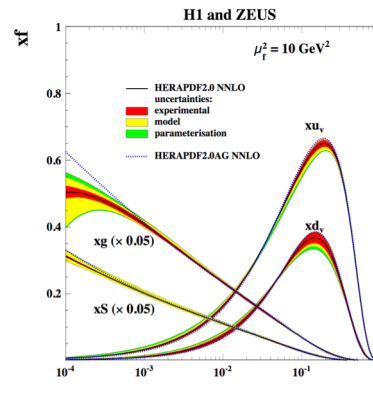


(Courtesy of A. Bacchetta)

Mapping the nucleon structure

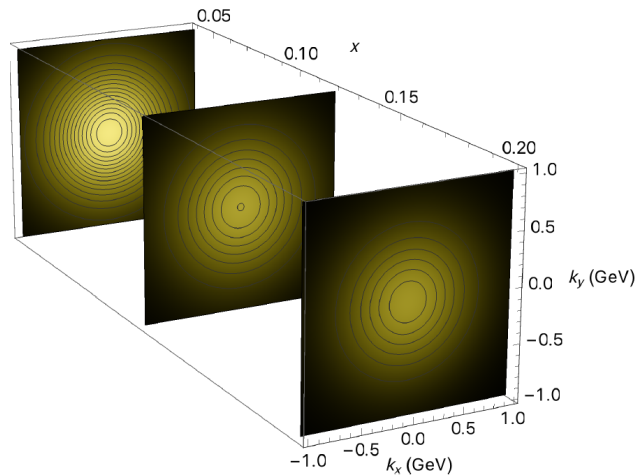
Collinear PDFs

1D



TMDs

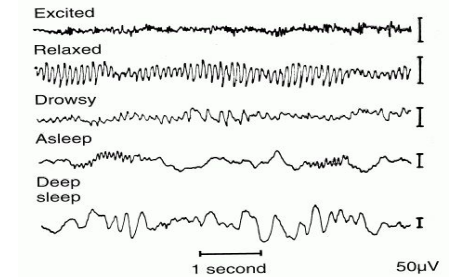
3D



(Courtesy of A. Bacchetta)

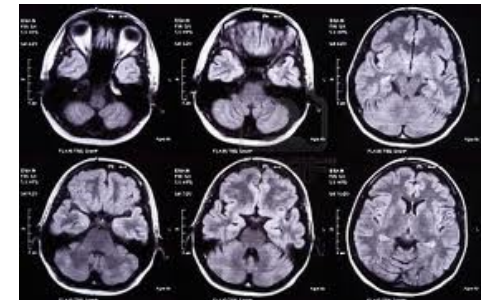
1D

electroencephalograms



3D

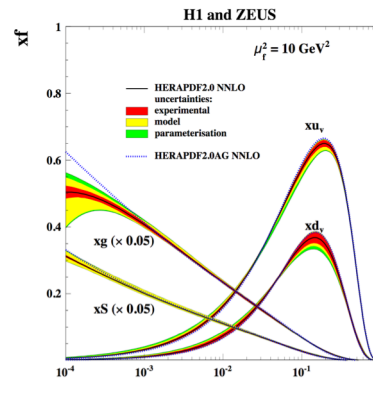
NMR imaging



Mapping the nucleon structure ...and more

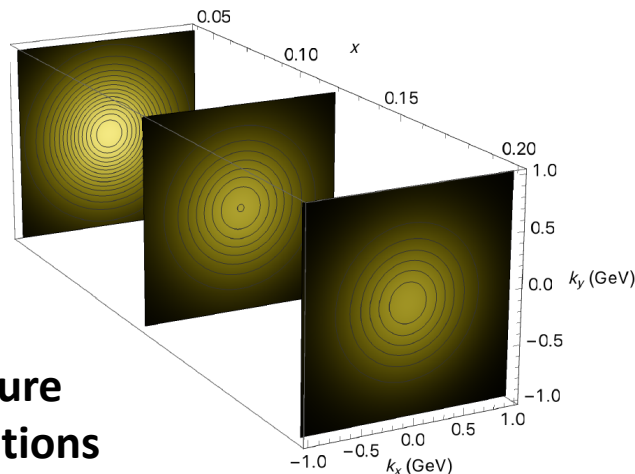
Collinear PDFs

1D



TMDs

3D

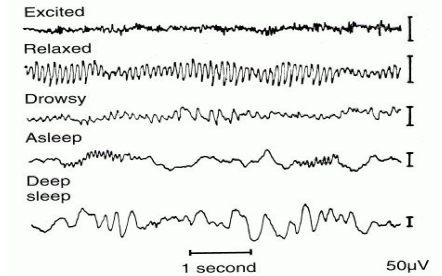


(Courtesy of A. Bacchetta)

- 3D maps of nucleon structure
- Describe spin-orbit correlations
- Are sensitive to the parton OAM
- T-odd TMDs are process dependent (breaking of QCD universality!)

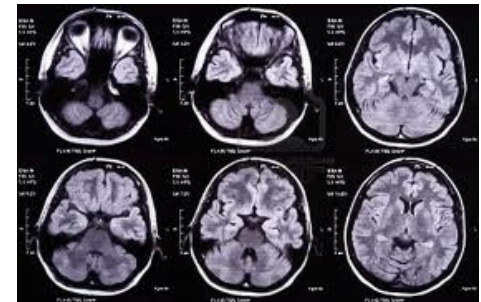
electroencephalograms

1D



3D

NMR imaging



The quark TMDs

		Quark TMDs		
		U	L	T
H a d r o n	U	f_1		h_1^\perp
	L		g_1	h_{1L}^\perp
	T	f_{1T}^\perp	g_{1T}^\perp	h_1

- 8 independent TMDs at twist-2
- Each with a probabilistic interpretation in terms of parton densities
- Significant experimental progress in the last 15 years!
- First extractions from global analyses

The quark TMDs

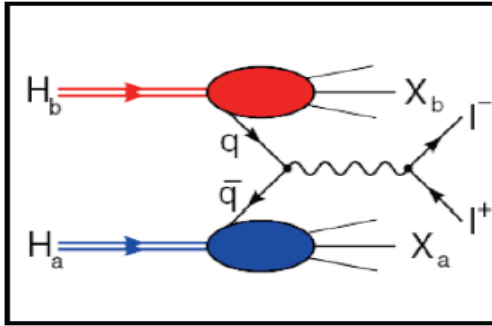
		Quark TMDs		
		U	L	T
H a d r o n	U	f_1		h_1^\perp
	L		g_1	h_{1L}^\perp
	T	f_{1T}^\perp	g_{1T}^\perp	h_1

- 8 independent TMDs at twist-2
- Each with a probabilistic interpretation in terms of parton densities
- Significant experimental progress in the last 15 years!
- First extractions from global analyses

- So far, main results obtained in **SIDIS** measurements (HERMES, COMPASS, JLAB)
- **Drell-Yan** in hadron-hadron collisions represents a complementary approach
- Unique kinematic region with fixed-target collisions at LHC
- Comparison of results from SIDIS and DY will allow to set stringent tests on QCD: factorization and universality

Probing the quark TMDs with a PGT at LHCb

Unpolarized Drell-Yan

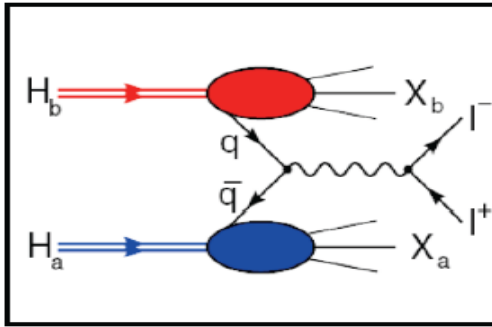


- Clean process
- LHCb has excellent reconstruction capabilities for $\mu\mu$ channel!

- Dominant process: $\bar{q}(x_{beam}) + q(x_{target}) \rightarrow \mu\mu$

Probing the quark TMDs with a PGT at LHCb

Unpolarized Drell-Yan



- Clean process
- LHCb has excellent reconstruction capabilities for $\mu\mu$ channel!

- Dominant process: $\bar{q}(x_{beam}) + q(x_{target}) \rightarrow \mu\mu$
- Provides sensitivity to unpolarized and BM TMDs

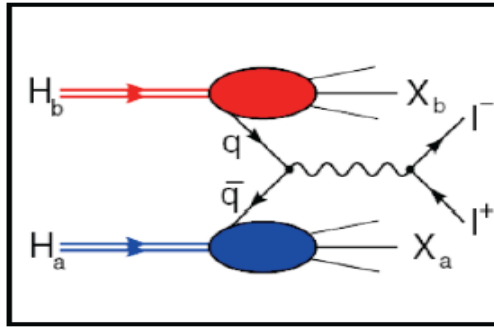
$$\sigma_{UU} \propto f_1 f_1 + \cos 2\phi h_1^\perp h_1^\perp$$

		Quark TMDs		
		U	L	T
H a d r o n	U	f_1		h_1^\perp
	L		g_1 -	h_{1L}^\perp -
	T	f_{1T}^\perp	g_{1T}^\perp -	h_1 - h_{1T}^\perp -

Boer-Mulders funct.
describes correlation
between transverse
spin and transverse
momentum of quarks
in unpol. nucleon

Probing the quark TMDs with a PGT at LHCb

Unpolarized Drell-Yan



- Clean process
- LHCb has excellent reconstruction capabilities for $\mu\mu$ channel!

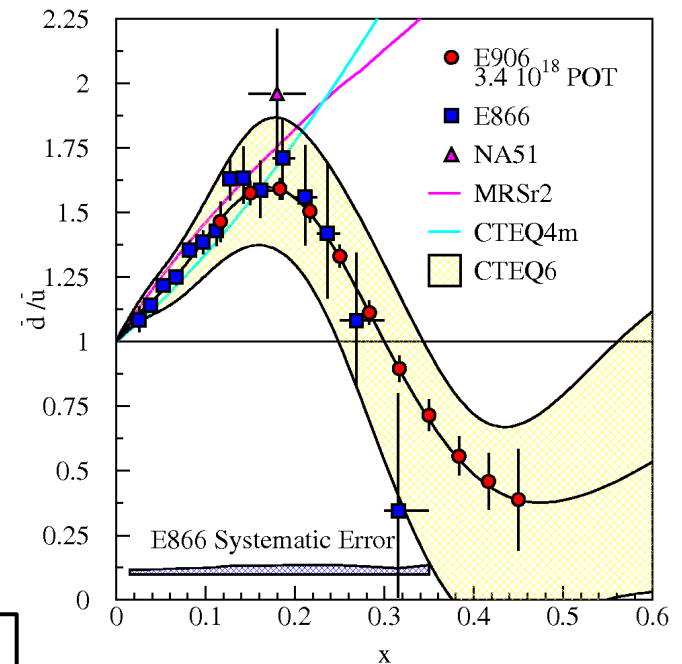
- Dominant process: $\bar{q}(x_{beam}) + q(x_{target}) \rightarrow \mu\mu$
- Provides sensitivity to unpolarized and BM TMDs

$$\sigma_{UU} \propto f_1 f_1 + \cos 2\phi h_1^\perp h_1^\perp$$

		Quark TMDs		
		U	L	T
H a d r o n	U	f_1		h_1^\perp
	L		g_1	h_{1L}^\perp
	T	f_{1T}^\perp	g_{1T}^\perp	h_{1T}^\perp

Boer-Mulders funct.
describes correlation between transverse spin and transverse momentum of quarks in unpol. nucleon

- Using fixed H and D targets allows to study the **antiquark content of the nucleon!**

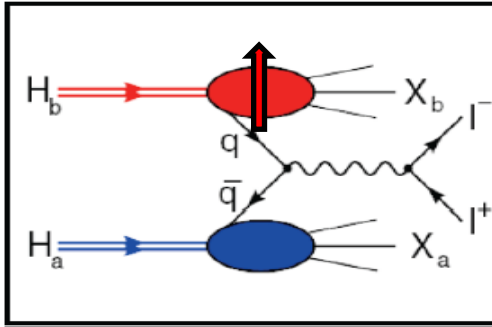


$$\bar{d}(x) \neq \bar{u}(x)!!$$

- hints that: $\bar{s}(x) \neq s(x)$
- **sea is not flavour symmetric!**
- **intrinsic sea quarks?**

Probing the quark TMDs with a PGT at LHCb

Polarized Drell-Yan

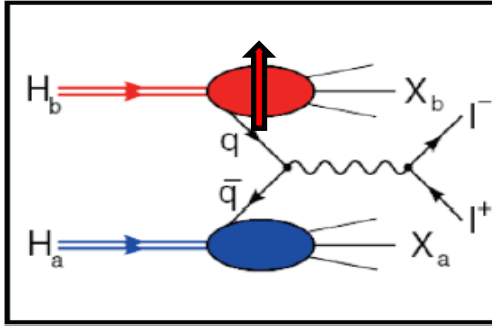


Sensitive to quark TMDs up to high x_2^\uparrow through TSSAs

$$A_N^{DY} = \frac{1}{P} \frac{\sigma_{DY}^\uparrow - \sigma_{DY}^\downarrow}{\sigma_{DY}^\uparrow + \sigma_{DY}^\downarrow}$$

Probing the quark TMDs with a PGT at LHCb

Polarized Drell-Yan



Sensitive to quark TMDs up to high x_2^\uparrow through TSSAs

$$A_N^{DY} = \frac{1}{P} \frac{\sigma_{DY}^\uparrow - \sigma_{DY}^\downarrow}{\sigma_{DY}^\uparrow + \sigma_{DY}^\downarrow}$$

$$A_{UT}^{\sin\phi_S} \sim \frac{f_1^q \otimes f_{1T}^{\perp q}}{f_1^q \otimes f_1^q}$$

$$A_{UT}^{\sin(2\phi+\phi_S)} \sim \frac{h_1^{\perp q} \otimes h_{1T}^{\perp q}}{f_1^q \otimes f_1^q}$$

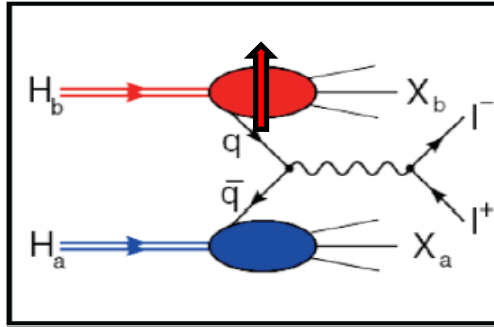
$$A_{UT}^{\sin(2\phi-\phi_S)} \sim \frac{h_1^{\perp q} \otimes h_1^q}{f_1^q \otimes f_1^q}$$

(ϕ : azimuthal orientation of lepton pair in dilepton CM)

		Quark TMDs		
		U	L	T
H a d r o n	U	f_1		h_1^\perp
	L		g_1	h_{1L}^\perp
	T	f_{1T}^\perp	g_{1T}^\perp	h_1

Probing the quark TMDs with a PGT at LHCb

Polarized Drell-Yan



Sensitive to quark TMDs up to high x_2^{\uparrow} through TSSAs

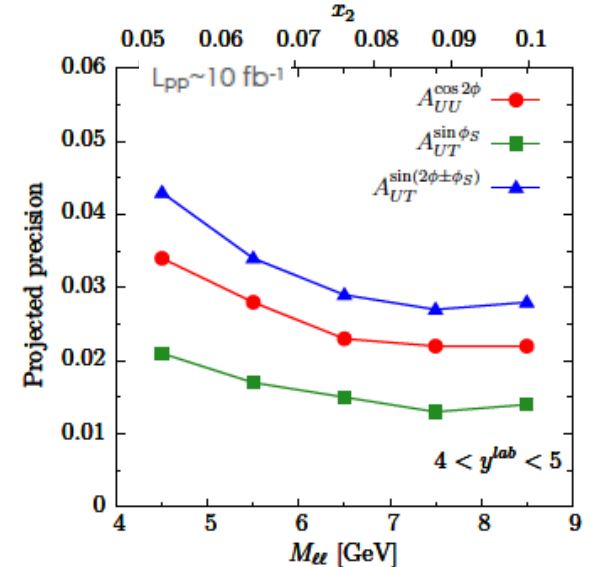
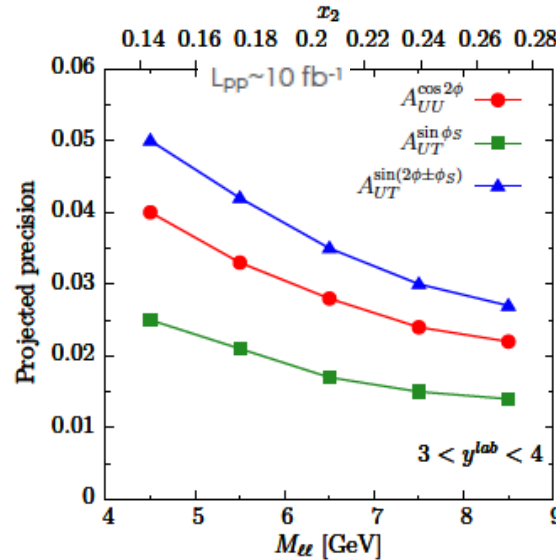
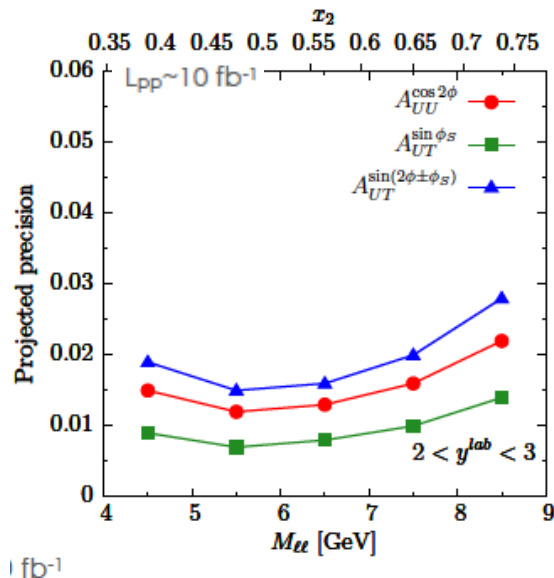
$$A_N^{DY} = \frac{1}{P} \frac{\sigma_{DY}^{\uparrow} - \sigma_{DY}^{\downarrow}}{\sigma_{DY}^{\uparrow} + \sigma_{DY}^{\downarrow}}$$

$$A_{UT}^{\sin\phi_S} \sim \frac{f_1^q \otimes f_{1T}^{\perp q}}{f_1^q \otimes f_1^q} \quad A_{UT}^{\sin(2\phi+\phi_S)} \sim \frac{h_1^{\perp q} \otimes h_{1T}^{\perp q}}{f_1^q \otimes f_1^q} \quad A_{UT}^{\sin(2\phi-\phi_S)} \sim \frac{h_1^{\perp q} \otimes h_1^q}{f_1^q \otimes f_1^q}$$


(ϕ : azimuthal orientation of lepton pair in dilepton CM)

arXiv:1807.00603

and J.P.Lansberg, PBC CERN 2018



Probing the gluon TMDs with a PGT at LHCb


		Gluon TMDs		
		Unpol	Circularly pol.	Linearly pol.
H a d r o n	U	f_1^g		$h_1^{\perp g}$
	L		g_1^g	$h_{1L}^{\perp g}$
	T	$f_{1T}^{\perp g}$	$g_{1T}^{\perp g}$	h_{1T}^g $h_{1T}^{\perp g}$

Theory framework consolidated

...but experimental access still extremely limited!

Note: gluons with non-zero p_T inside an unpolarized hadron can be linearly polarized!

Probing the gluon TMDs with a PGT at LHCb

		Gluon TMDs		
		Unpol	Circularly pol.	Linearly pol.
H a d r o n	U	f_1^g		$h_1^{\perp g}$
	L		g_1^g	$h_{1L}^{\perp g}$
	T	$f_{1T}^{\perp g}$	$g_{1T}^{\perp g}$	h_{1T}^g $h_{1T}^{\perp g}$

Theory framework consolidated

...but experimental access still extremely limited!

Note: gluons with non-zero p_T inside an unpolarized hadron can be linearly polarized!

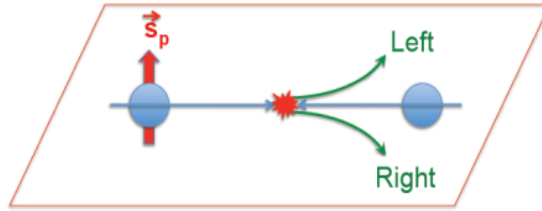
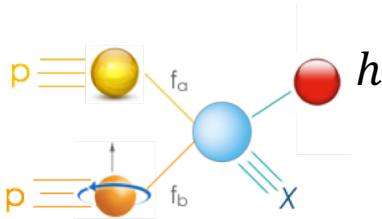
Gluon Sivers function:

- sheds light on spin-orbit correlations of gluons inside the proton
- sensitive to gluon orbital angular momentum!
- first hints by RHIC and COMPASS, but still basically unknown!

Probing the gluon TMDs with a PGT at LHCb

Main observables in pol. hadron collisions: **Single Transverse Spin Asymmetries (TSSAs)**

Polarized inclusive hard scattering

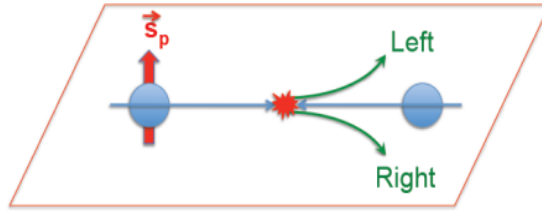
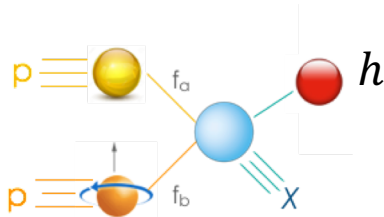


$$A_N = \frac{1}{P} \frac{\sigma^\uparrow - \sigma^\downarrow}{\sigma^\uparrow + \sigma^\downarrow} \sim \frac{1}{P} \frac{N_h^\uparrow - N_h^\downarrow}{N_h^\uparrow + N_h^\downarrow}$$

Probing the gluon TMDs with a PGT at LHCb

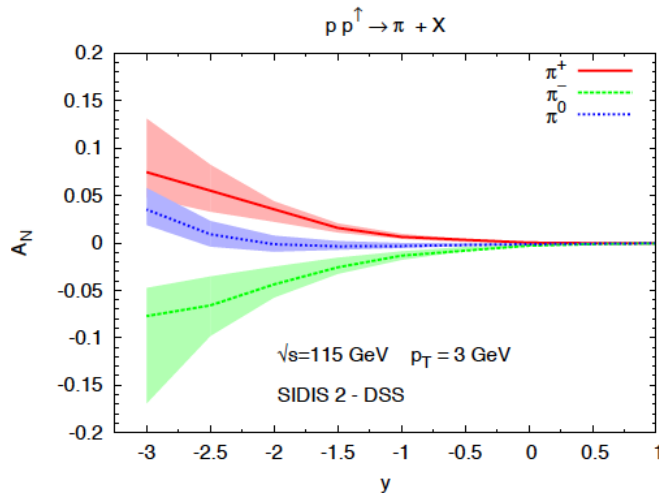
Main observables in pol. hadron collisions: **Single Transverse Spin Asymmetries (TSSAs)**

Polarized inclusive hard scattering

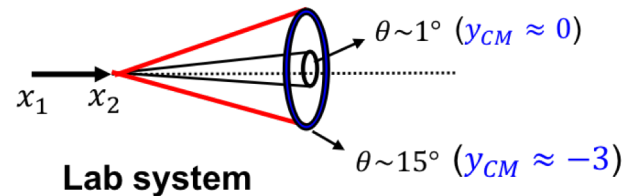


$$A_N = \frac{1}{P} \frac{\sigma^\uparrow - \sigma^\downarrow}{\sigma^\uparrow + \sigma^\downarrow} \sim \frac{1}{P} \frac{N_h^\uparrow - N_h^\downarrow}{N_h^\uparrow + N_h^\downarrow}$$

Anselmino et al. [arXiv:1504.03791v2](https://arxiv.org/abs/1504.03791v2)



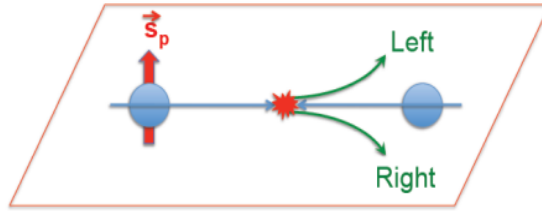
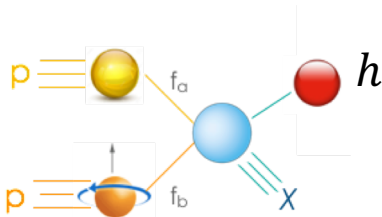
- **Asymmetries above 10 %! Big signature!!**
- The effect increases with more negative CM rapidity
- Nicely matches the LHCb acceptance with fixed target at LHC



Probing the gluon TMDs with a PGT at LHCb

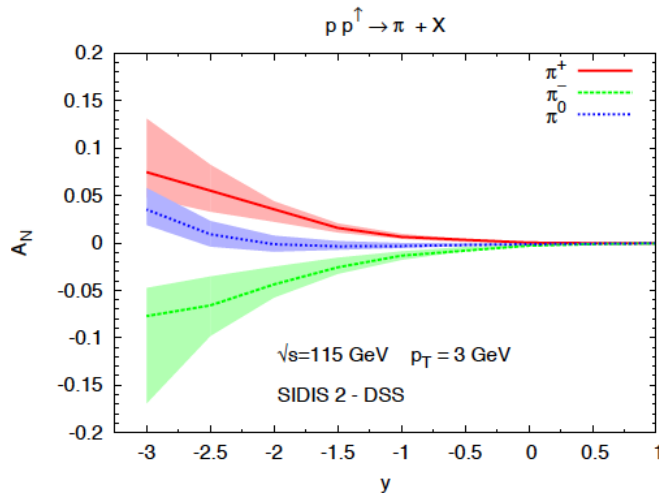
Main observables in pol. hadron collisions: **Single Transverse Spin Asymmetries (TSSAs)**

Polarized inclusive hard scattering

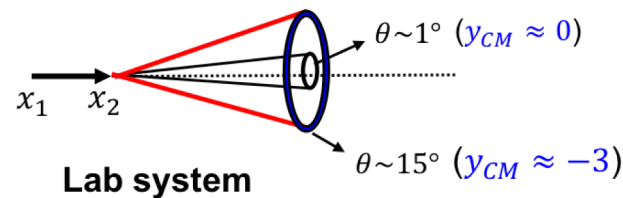


$$A_N = \frac{1}{P} \frac{\sigma^\uparrow - \sigma^\downarrow}{\sigma^\uparrow + \sigma^\downarrow} \sim \frac{1}{P} \frac{N_h^\uparrow - N_h^\downarrow}{N_h^\uparrow + N_h^\downarrow}$$

Anselmino et al. [arXiv:1504.03791v2](https://arxiv.org/abs/1504.03791v2)



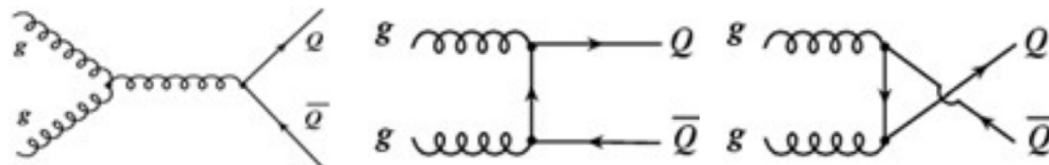
- **Asymmetries above 10 %! Big signature!!**
- The effect increases with more negative CM rapidity
- Nicely matches the LHCb acceptance with fixed target at LHC



- Inclusive pion production provides mainly sensitivity to the quark PDFs.
- **The most efficient way to get sensitivity to the gluon PDFs is through heavy-flavour observables.**

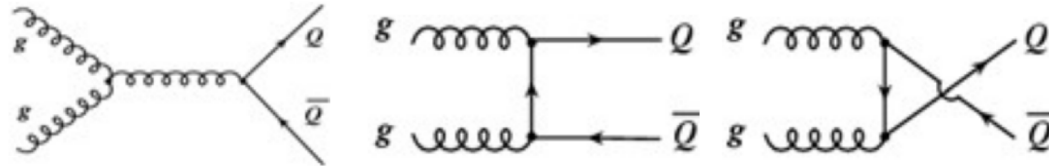
Probing the gluon TMDs with a PGT at LHCb

In high-energy hadron collisions heavy quarks dominantly produced through gg interactions:

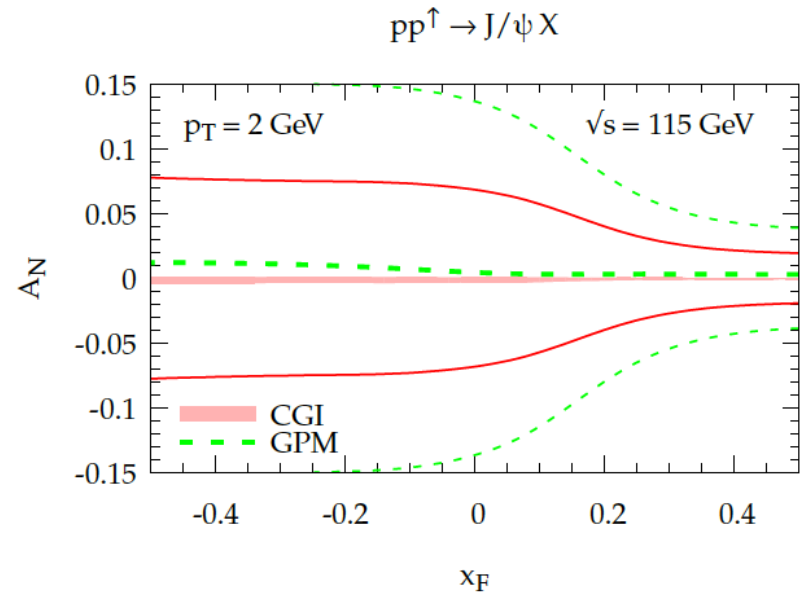
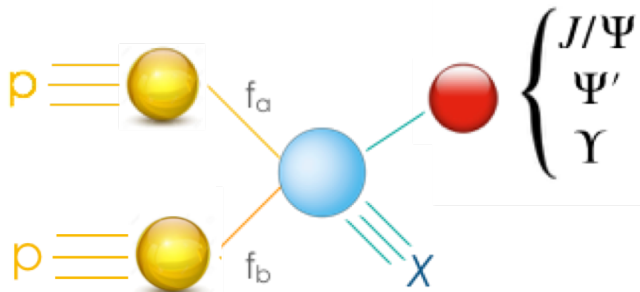


Probing the gluon TMDs with a PGT at LHCb

In high-energy hadron collisions heavy quarks dominantly produced through gg interactions:



Inclusive quarkonia production in pp interaction turns out to be an ideal **gluon-sensitive observable**!



Phys. Rev. D 99, 036013 (2019)

Probing the gluon TMDs with a PGT at LHCb

The measured TSSAs can be related to the convolution of the gluon Sivers function for the target proton and the unpolarized gluon pdf for the beam proton:

$$A_N = \frac{1}{P} \frac{\sigma^\uparrow - \sigma^\downarrow}{\sigma^\uparrow + \sigma^\downarrow} \sim \frac{1}{P} \frac{N_h^\uparrow - N_h^\downarrow}{N_h^\uparrow + N_h^\downarrow} \propto [f_{1T}^{\perp g}(x_a, k_{\perp a}) \otimes f_g(x_b, k_{\perp b}) \otimes d\sigma_{gg \rightarrow QQg}] \sin \phi_S + \dots$$

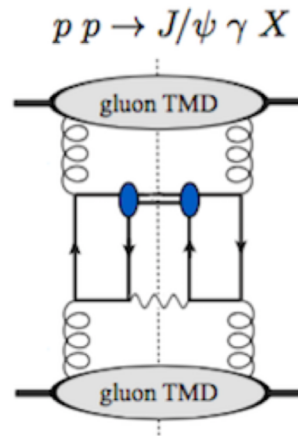
Probing the gluon TMDs with a PGT at LHCb

The measured TSSAs can be related to the convolution of the gluon Siverts function for the target proton and the unpolarized gluon pdf for the beam proton:

$$A_N = \frac{1}{P} \frac{\sigma^\uparrow - \sigma^\downarrow}{\sigma^\uparrow + \sigma^\downarrow} \sim \frac{1}{P} \frac{N_h^\uparrow - N_h^\downarrow}{N_h^\uparrow + N_h^\downarrow} \propto [f_{1T}^{\perp g}(x_a, k_{\perp a}) \otimes f_g(x_b, k_{\perp b}) \otimes d\sigma_{gg \rightarrow QQg}] \sin \phi_S + \dots$$

Caveat: TMD factorization requires $p_T(Q) \ll M_Q$. At LHC one can look at **back-to-back production of quarkonia and isolated photon or associate quarkonia production**, where only the relative p_T has to be small:

$$pp \rightarrow J/\psi + \gamma + X \quad pp \rightarrow \Upsilon + \gamma + X \quad pp \rightarrow J/\psi + J/\psi + X$$

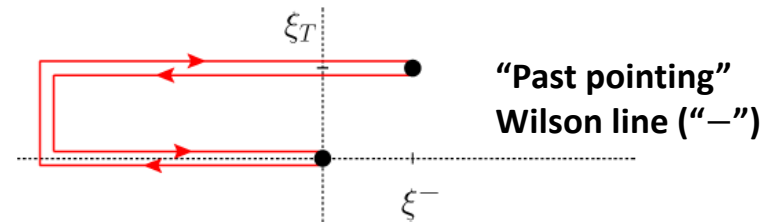
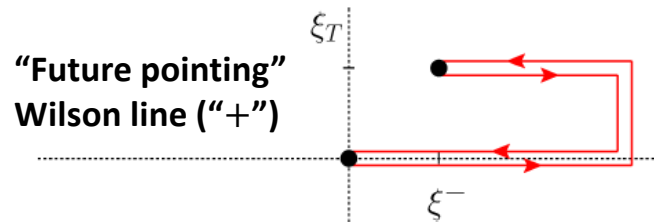


Probing the gluon PDFs

As for quark TMDs, also the gluon TMD phenomenology is enriched by the **process dependence** originating from ISI/FSI and encoded in the **gauge links**.

The gluon correlator depends on two path-dependent gauge links [D. Boer: [arXiv:1611.06089](https://arxiv.org/abs/1611.06089)]

$$\Gamma^{\mu\nu}[\mathcal{U}, \mathcal{U}'](x, \mathbf{k}_T) \equiv \int \frac{d(\xi \cdot P) d^2 \xi_T}{(P \cdot n)^2 (2\pi)^3} e^{i(xP + k_T) \cdot \xi} \langle P | \text{Tr}_c \left[F^{n\nu}(0) \boxed{\mathcal{U}_{[0, \xi]}} F^{n\mu}(\xi) \boxed{\mathcal{U}'_{[\xi, 0]}} \right] | P \rangle$$

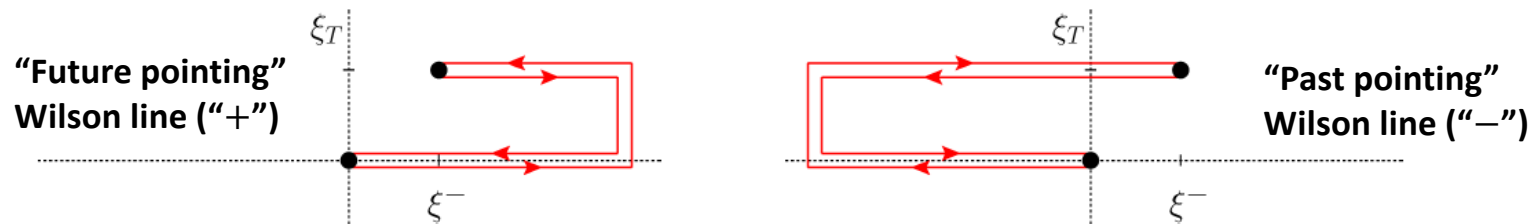


Probing the gluon PDFs

As for quark TMDs, also the gluon TMD phenomenology is enriched by the **process dependence** originating from ISI/FSI and encoded in the **gauge links**.

The gluon correlator depends on two path-dependent gauge links [D. Boer: [arXiv:1611.06089](https://arxiv.org/abs/1611.06089)]

$$\Gamma^{\mu\nu}[\mathcal{U}, \mathcal{U}'](x, \mathbf{k}_T) \equiv \int \frac{d(\xi \cdot P) d^2 \xi_T}{(P \cdot n)^2 (2\pi)^3} e^{i(xP + k_T) \cdot \xi} \langle P | \text{Tr}_c \left[F^{n\nu}(0) \mathcal{U}_{[0, \xi]} F^{n\mu}(\xi) \mathcal{U}'_{[\xi, 0]} \right] | P \rangle$$



Both f_1^g and $h_1^{\perp g}$ are process dependent! Each of them can be of two types:

$[+ +] = [- -]$ Weizsacker-Williams (WW) $[+ -] = [- +]$ DiPole (DP)

- can differ in magnitude and width (!)
- can be probed by different processes

Probing the gluon PDFs

[D. Boer: [arXiv:1611.06089](https://arxiv.org/abs/1611.06089)]

	DIS	DY	SIDIS	$pA \rightarrow \gamma \text{ jet } X$	$ep \rightarrow e' Q \bar{Q} X$ $ep \rightarrow e' j_1 j_2 X$	$pp \rightarrow \eta_{c,b} X$ $pp \rightarrow H X$	$pp \rightarrow J/\psi \gamma X$ $pp \rightarrow \Upsilon \gamma X$
$f_1^g^{[+,+]} (WW)$	×	×	×	×	✓	✓	✓
$f_1^g^{[+,-]} (DP)$	✓	✓	✓	✓	×	×	×

	$pp \rightarrow \gamma \gamma X$	$pA \rightarrow \gamma^* \text{ jet } X$	$ep \rightarrow e' Q \bar{Q} X$ $ep \rightarrow e' j_1 j_2 X$	$pp \rightarrow \eta_{c,b} X$ $pp \rightarrow H X$	$pp \rightarrow J/\psi \gamma X$ $pp \rightarrow \Upsilon \gamma X$
$h_1^{\perp g [+,+]} (WW)$	✓	×	✓	✓	✓
$h_1^{\perp g [+, -]} (DP)$	×	✓	×	×	×



Can be measured at the EIC



Can be measured at the LHC (and in particular at LHCb with SMOG2)

Process dependence of the GSF

Two independent gluon Sivers functions can be defined from the different combinations of Wilson lines in the gluon correlator:

$f_{1T}^{\perp g[+,+]}$ “**f-type**” → antisymmetric colour structures

$f_{1T}^{\perp g[+,-]}$ “**d-type**” → symmetric colour structures

Can differ in magnitude and width (!)

Can be probed by different processes:

[D. Boer: [arXiv:1611.06089](https://arxiv.org/abs/1611.06089), D. Boer et al. HEPJ 08 2016 001]

	DY	SIDIS	$p^\dagger A \rightarrow h X$	$p^\dagger A \rightarrow \gamma^{(*)} \text{jet } X$	$p^\dagger p \rightarrow \gamma \gamma X$ $p^\dagger p \rightarrow J/\psi \gamma X$ $p^\dagger p \rightarrow J/\psi J/\psi X$	$ep^\dagger \rightarrow e' Q \bar{Q} X$ $ep^\dagger \rightarrow e' j_1 j_2 X$
$f_{1T}^{\perp g[+,+]} \text{ (WW)}$	×	×	×	×	✓	✓
$f_{1T}^{\perp g[+,-]} \text{ (DP)}$	✓	✓	✓	✓	×	×

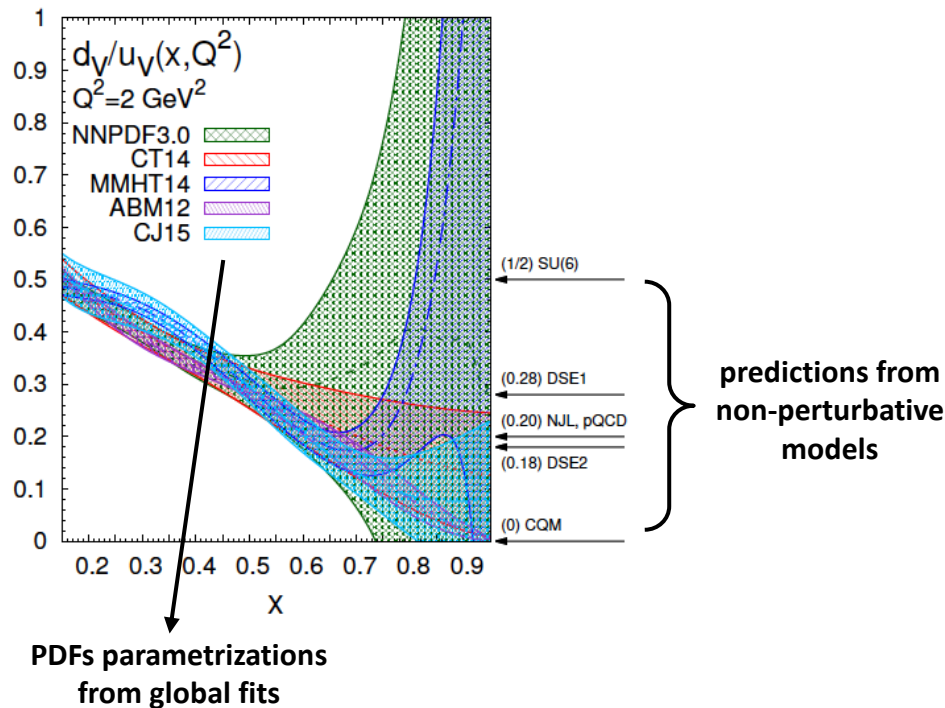
Can be measured at the EIC
 Can be measured at the LHCb with a PGT

$$[+, +] \longleftrightarrow f_{1T}^{\perp g[ep^\dagger \rightarrow e' Q \bar{Q} X]}(x, p_T^2) = -f_{1T}^{\perp g[p^\dagger p \rightarrow \gamma \gamma X]}(x, p_T^2) \longleftrightarrow [-, -]$$

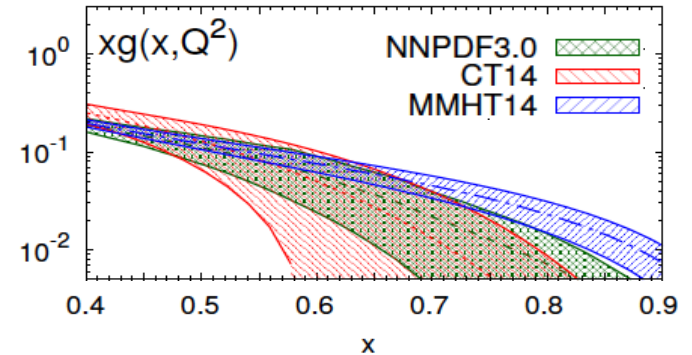
Same sign-change relation expected for the other T-odd gTMDs h_1^g and $h_{1T}^{\perp g}$!

The high- x frontier

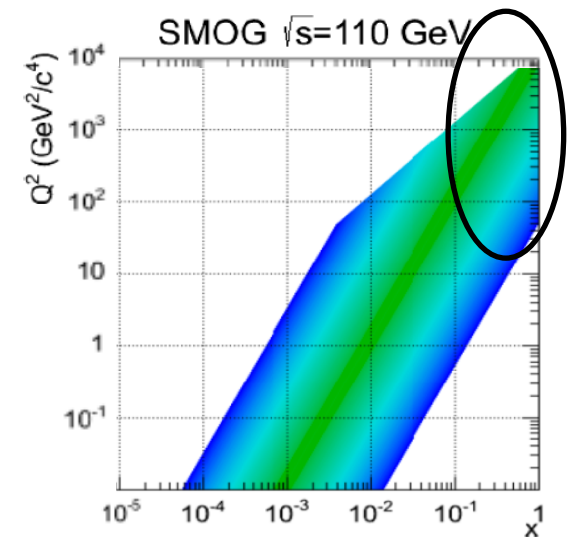
[R. D. Ball et al. Eur. Phys. J. C76 (2016) 383]



Fermi motion in the nucleus can allow to access the **exotic $x > 1$ region**, where parton dynamics depends on the interaction between the nucleons within the nucleus (unexplored bridge between QCD and nuclear physics!)

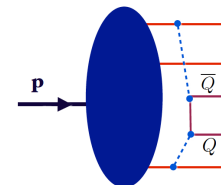


- Huge uncertainties at very large x
- **Quest for data at $x > 0.5$**
- $q(x_{\text{targ}})$ with H and D at SMOG2



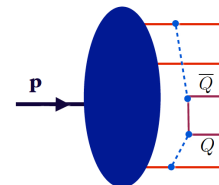
More physics reach with unpolarized FT reactions

- **Intrinsic heavy-quark** [S.J. Brodsky et al., Adv.High Energy Phys. 2015 (2015) 231547]
 - 5-quark Fock state of the proton may contribute at high x !
 - **charm PDFs** at large x could be larger than obtained from conventional fits



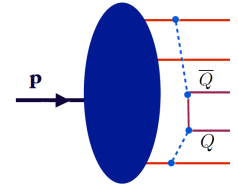
More physics reach with unpolarized FT reactions

- **Intrinsic heavy-quark** [S.J. Brodsky et al., Adv.High Energy Phys. 2015 (2015) 231547]
 - 5-quark Fock state of the proton may contribute at high x !
 - **charm PDFs** at large x could be larger than obtained from conventional fits
- **pA collisions** (using unpolarized gas: He, N, Ne, Ar, Kr, Xe)
 - constraints on nPDFs (e.g. on poorly understood **gluon antishadowing at high x**)
 - studies of parton energy-loss and absorption phenomena in the cold medium

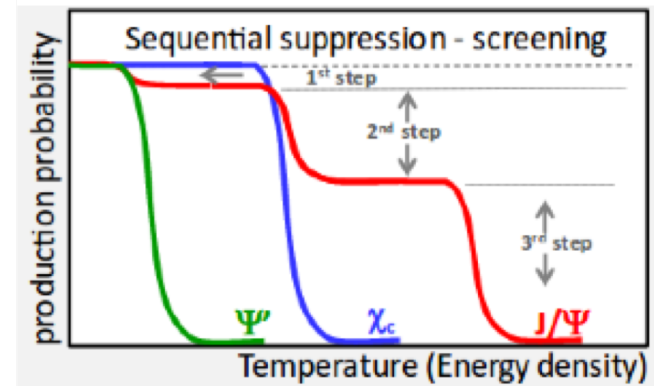
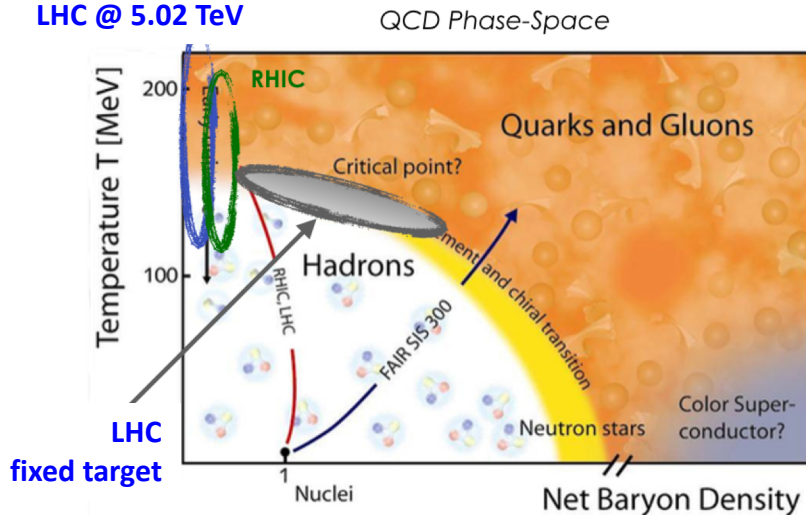


More physics reach with unpolarized FT reactions

- **Intrinsic heavy-quark** [S.J. Brodsky et al., Adv.High Energy Phys. 2015 (2015) 231547]
 - 5-quark Fock state of the proton may contribute at high x !
 - **charm PDFs** at large x could be larger than obtained from conventional fits
- **pA collisions** (using unpolarized gas: He, N, Ne, Ar, Kr, Xe)
 - constraints on nPDFs (e.g. on poorly understood **gluon antishadowing at high x**)
 - studies of parton energy-loss and absorption phenomena in the cold medium
- **PbA collisions at $\sqrt{s_{NN}} \approx 72$ GeV** (using unpolarized gas: He, N, Ne, Ar, Kr, Xe)
 - Study of **QGP formation** (search for predicted **sequential quarkonium suppression**)



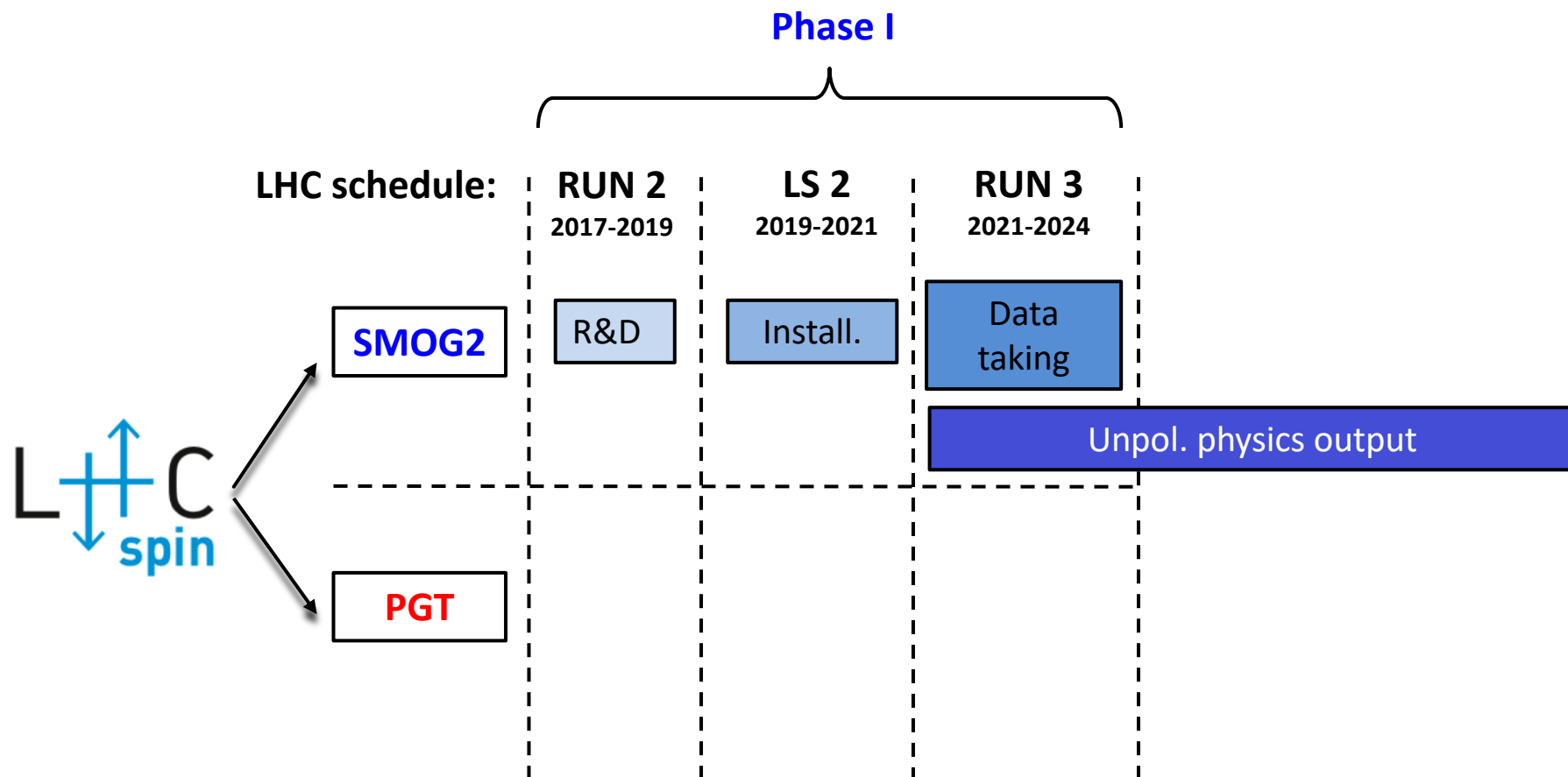
LHC @ 5.02 TeV



$c\bar{c}$ states: $J/\psi, \chi_c, \psi', \dots$

Different binding energy, different dissociation temp.

Time schedule of the project



Time schedule of the project

